


Whole exome sequencing identifies the potential for genetic rescue in iconic and critically endangered Panamanian harlequin frogs

Allison Q. Byrne^{1,2}  | Corinne L. Richards-Zawacki³ | Jamie Voyles⁴ | Ke Bi² | Roberto Ibáñez^{5,6} | Erica Bree Rosenblum^{1,2}

¹Department of Environmental Science, Policy, and Management, University of California Berkeley, Berkeley, CA, USA

²Museum of Vertebrate Zoology, University of California Berkeley, Berkeley, CA, USA

³Department of Biological Sciences, University of Pittsburgh, Pittsburgh, PA, USA

⁴Department of Biology, University of Nevada Reno, Reno, NV, USA

⁵Smithsonian Tropical Research Institute, Panamá, República de Panamá

⁶Sistema Nacional de Investigación, SENACYT, Clayton, Panamá, República de Panamá

Correspondence

Allison Q. Byrne, Department of Environmental Science, Policy, and Management, University of California Berkeley, Berkeley, CA, USA.
Email: allie128@berkeley.edu

Funding information

Association of Zoos and Aquariums; Division of Graduate Education, Grant/Award Number: GRFP; Division of Environmental Biology, Grant/Award Number: 1457694, 1551488, 1660311 and 1846403; Disney Worldwide Conservation Fund

Abstract

Avoiding extinction in a rapidly changing environment often relies on a species' ability to quickly adapt in the face of extreme selective pressures. In Panamá, two closely related harlequin frog species (*Atelopus varius* and *Atelopus zeteki*) are threatened with extinction due to the fungal pathogen *Batrachochytrium dendrobatidis* (*Bd*). Once thought to be nearly extirpated from Panamá, *A. varius* have recently been rediscovered in multiple localities across their historical range; however, *A. zeteki* are possibly extinct in the wild. By leveraging a unique collection of 186 *Atelopus* tissue samples collected before and after the *Bd* outbreak in Panama, we describe the genetics of persistence for these species on the brink of extinction. We sequenced the transcriptome and developed an exome-capture assay to sequence the coding regions of the *Atelopus* genome. Using these genetic data, we evaluate the population genetic structure of historical *A. varius* and *A. zeteki* populations, describe changes in genetic diversity over time, assess the relationship between contemporary and historical individuals, and test the hypothesis that some *A. varius* populations have rapidly evolved to resist or tolerate *Bd* infection. We found a significant decrease in genetic diversity in contemporary (compared to historical) *A. varius* populations. We did not find strong evidence of directional allele frequency change or selection for *Bd* resistance genes, but we uncovered a set of candidate genes that warrant further study. Additionally, we found preliminary evidence of recent migration and gene flow in one of the largest persisting *A. varius* populations in Panamá, suggesting the potential for genetic rescue in this system. Finally, we propose that previous conservation units should be modified, as clear genetic breaks do not exist beyond the local population level. Our data lay the groundwork for genetically informed conservation and advance our understanding of how imperiled species might be rescued from extinction.

KEYWORDS

amphibians, conservation, disease, exome capture, extinction, genetic rescue

1 | INTRODUCTION

Extinction is a pressing threat for many species on Earth. A myriad of stressors—including climate change, habitat destruction, invasive species, and infectious disease—drive reductions in population sizes and decrease connectivity, often leading small populations toward an “extinction vortex” (Gilpin & Soule, 1986). This vortex is caused in part by the vulnerability of small populations to environmental and demographic stochasticity (Shaffer, 1981). In addition, erosion of genetic diversity also plays a key role in this process. Inbreeding depression, which leads to a loss of genetic diversity and an increase in the expression of deleterious genetic variants, is a significant contributor to extinction risk in small, isolated populations (Frankham, 2005). Problems associated with inbreeding depression can also apply to ex situ captive breeding efforts, where small founding populations are brought into captivity and inbred, decreasing the chances of successful reintroductions in the future (Hedrick & Garcia-Dorado, 2016). Therefore, understanding the genetics of population declines is critical to understanding extinction risk and making informed conservation decisions.

In addition to providing key insights into population declines, genetic and genomic techniques can also help reveal mechanisms underlying persistence and recovery of natural populations. There are a few non-mutually exclusive processes by which natural populations may be rescued from extinction. First, demographic rescue refers to the simple addition of individuals to a population via immigration and the subsequent boost in population size which can prevent extinction (Brown & Kodric-Brown, 1977). Second, genetic rescue refers to the positive effect of increased gene flow in small, threatened populations—over and above what can be attributed to the demographic effect of adding migrants (Ingvarsson, 2001). The positive effects of genetic rescue are the product of a reduction of genetic load (high frequency of deleterious genetic variants), and the high fitness of hybrid individuals (Tallmon et al., 2004). Third, evolutionary rescue occurs when populations undergo rapid adaptive evolution via natural selection (Gomulkiewicz & Holt, 1995; Gonzalez et al., 2013). The probability of evolutionary rescue as a means of population recovery is highest for populations with large initial sizes, low levels of initial maladaptation to particular environmental conditions, and high levels of standing genetic variation (Carlson et al., 2014). In practice, little is known about which of these mechanisms contribute to recoveries of species on the brink of extinction.

One clade that has suffered particularly alarming declines is the neotropical harlequin frogs (genus *Atelopus*), due in large part to the devastating amphibian chytrid fungus *Batrachochytrium dendrobatidis* (*Bd*; Longcore et al., 1999; La Marca et al., 2005). It was estimated that from 1970 to 2002, 81% of *Atelopus* species declined and only 12% had stable populations (La Marca et al., 2005). Despite early evidence suggesting a dire outcome, some *Atelopus* species have persisted in small populations within their historical range in Costa Rica (González-Maya et al., 2013), Venezuela (Rodríguez-Contreras et al., 2008), Ecuador (Barrio-Amorós et al., 2020; Tapia et al., 2017), and Panamá (Perez et al., 2014; Voyles et al., 2018). However, these

populations are often small and isolated, in some cases show evidence of low recruitment (González-Maya et al., 2018), and thus may still be at high risk of extinction. Persistent populations offer a unique opportunity to investigate mechanisms of host resistance or tolerance to *Bd* infection and disease development in this severely imperiled amphibian clade.

One intriguing case study of rapid decline and persistence is the critically endangered *Atelopus varius* in Panamá (Voyles et al., 2018). This species, along with the closely related Panamanian Golden Frog (*Atelopus zeteki*), declined precipitously after *Bd* swept through Panamá in the early 2000's (Crawford et al., 2010). These two species, which together form a monophyletic clade (Ramírez et al., 2020; Richards & Knowles, 2007) have garnered significant interest and funding to mitigate population losses, owing in part to their charismatic appearance, historical ubiquity, and cultural significance in Panamá (Poole, 2008). Conservation interventions have included forming robust captive colonies in Panamá and in zoos across the United States (Gagliardo et al., 2008). While captive populations of *A. zeteki* and *A. varius* are considered secure (Lewis et al., 2019), a recent reintroduction attempt was not successful in re-establishing wild populations of *A. varius* (Panamá Amphibian Rescue and Conservation Project, 2018). *Bd* is enzootic and widespread in Panama, making the reintroduction of susceptible species exceedingly difficult (Voyles et al., 2018). Integrating studies of persistent wild populations into captive management decisions could be key to improving future ex-situ conservation efforts.

Previous research suggests that host-specific processes might be responsible for the persistence of some *Atelopus* species in Panamá. Initial laboratory studies showed that *A. zeteki* is highly susceptible to *Bd* (Bustamante et al., 2010). *Bd* infection intensity typically increases rapidly often leading to mortality (DiRenzo et al., 2014), which may be due to *Bd*'s ability to suppress host immune defenses (Ellison et al., 2014), a lack of protective microbial symbionts on host skin (Becker et al., 2015), and/or ineffectiveness of secreted antimicrobial peptides (Woodhams et al., 2006). Other studies have found that the virulence of *Bd* in Panamá has not changed since the pathogen's arrival, indicating that attenuating pathogen virulence is not driving host persistence (Voyles et al., 2018). Considering possible environmental mediators of persistence, studies have found that *A. varius* persist in many different microclimates (i.e., warmer lowlands and cooler highlands; Perez et al., 2014), indicating that shared environmental refugia likely do not explain persistence in these species. Finally, there is evidence that persisting *A. varius* skin secretions are better at inhibiting *Bd* growth than secretions from *A. varius* brought into captivity before *Bd* arrival (Voyles et al., 2018). Given the lack of evidence indicating environmental or pathogen-mediated shifts predicting changes in survival, and noting preliminary evidence of increased host defenses against *Bd*, we use a genomic approach to investigate the hypothesis that changes in the amphibians themselves may underlie persistence.

In this study, we designed a genomic capture assay to sequence the expressed, functional regions of the *Atelopus* genome (Bi et al., 2012). With this exome capture assay, we sequenced *A. varius*

and *A. zeteki* samples collected from across their historical range in Panamá and from the captive colonies at the Panamá Amphibian Rescue and Conservation Project (PARC). We also sequenced contemporary individuals from persisting populations. Our contemporary samples represent a significant re-survey effort of historical *A. varius/zeteki* sites across their entire historical range in Panama. Our captive samples represent all distinct *A. varius/zeteki* lineages currently in captivity in Panamá. Leveraging our paired time series data, we seek to (a) evaluate the population genetic structure of historical *A. varius* and *A. zeteki* in Panamá (b) compare the genetic diversity of historical, contemporary, and captive populations and (c) scan the coding regions of the *A. varius* genome to search for genetic variants linked to persistence in the face of ongoing disease threats. Together, addressing these objectives will advance our understanding of what demographic and/or adaptive processes contribute to host persistence and facilitate data-driven conservation efforts.

2 | METHODS

2.1 | Sample collection

Our study included 190 samples, with 130 historical (2001–2004), 39 contemporary (2012–2016), 17 captive, and 4 Costa Rican *Atelopus* samples (see Table S1). We collected historical samples before the *Bd* outbreak in Panamá as described in Richards and Knowles (2007). For contemporary samples, we conducted field surveys between 2012 and 2016 as described in Voyles et al. (2018). Briefly, we conducted visual encounter surveys during both the dry season (December–January) and wet season (May–July) at stream sites that were previously known to have *A. varius* or *A. zeteki* populations. We conducted surveys on 200 m stream transects where two to three observers walked the length of the transect slowly searching for amphibians. We captured *A. varius* adults with a pair of fresh gloves and collected skin swabs for *Bd* detection and a toe clip sample for genetic analysis. We collected DNA samples from captive individuals via buccal swab at the El Valle Amphibian Conservation Center (EVACC). Finally, we sourced four DNA samples from the Museum of Vertebrate Zoology frozen tissue collection: MVZ149729: *Atelopus varius* collected in Costa Rica 1976, MVZ149734: *Atelopus senex* collected in Costa Rica in 1976, MVZ223270: *Atelopus chiriquiensis* collected in Costa Rica in 1990, MVZ223280: *Atelopus varius* collected in Costa Rica in 1990.

2.2 | qPCR for *Bd*

To test for the presence of *Bd* in contemporary *A. varius* samples, skin swabs were also collected. Genomic DNA was extracted using Qiagen DNeasy Blood and Tissue kit following the manufacturer's protocol for animal tissue. We used a quantitative polymerase chain reaction (qPCR) assay to quantify *Bd* DNA (Boyle et al., 2004; Hyatt et al., 2007). Each qPCR was run in triplicate and included positive

and negative controls and a sevenfold dilution series of plasmid-based *Bd* standards (Pisces Molecular). Samples that had >1 *Bd* DNA copies in at least one reaction were considered positive. Finally, we converted average *Bd* DNA copy number per 5 µl reaction volume to whole-swab loads.

2.3 | Exome capture design

Genomes for the focal species were not available a priori, so we sequenced transcriptomes to design our capture assay. To maximize transcript discovery, we extracted RNA from three captive-bred *A. varius* at varying stages of *Bd* infection (uninfected, early infected, late infected) using four different tissue types (liver, spleen, dorsal skin, ventral skin). All animals were euthanized by rapid decapitation followed by double pithing in accordance with the Tulane University IACUC protocol 0453. RNA was extracted using a Trizol protocol (Rio et al., 2010) with some minor modifications. First, we homogenized the tissue using 2.8 mm ceramic beads and 500 µl of Trizol with MoBio PowerLyzer at the recommended setting for animal tissues. We then incubated the homogenized tissue and Trizol in a Heavy Phase-Lock Gel tube for 5 min at room temperature. After extraction, we treated RNA samples with Turbo DNAase (Ambion). RNA was quantified using Qubit and quality was assessed using the Agilent bioanalyzer. All RNA extractions had an RNA integrity number (RIN) of at least 7 (Schroeder et al., 2006). For library preparation, we sent samples to IBEST Genomics Resources Core at the University of Idaho, where they performed an Apollo Poly mRNA select and Illumina strand RNA library prep. Samples were then sequenced at the QB3 Vincent J. Coates Genomics Sequencing Laboratory at UC Berkeley on one lane of an Illumina HiSeq 4000 using the 150 paired end kit.

Next, we combined our sequence data to create a single assembled transcriptome for probe design. First, we cleaned reads following Bi et al. (2012) and Singhal (2013) and assembled reads using TRINITY (Grabherr et al., 2011). We then selected the longest transcript per TRINITY gene and annotated them with *Nanorana parkeri*, *Xenopus tropicalis*, and *Anolis carolinensis* protein reference using BLASTX (Altschul et al., 1997) and EXONERATE (Slater & Birney, 2005). Fragmented transcripts that hit to the same reference protein were joined by Ns according to their relative BLAST hit positions. The resulting transcripts were then combined to remove redundancies via Cd-hit-est (Li & Godzik, 2006) and CAP3 (Huang & Madan, 1999). We defined coding sequences (cds) of each annotated transcript using EXONERATE and specified these regions in a bed format. The pipelines used for transcriptome data processing and annotation are available at <https://github.com/CGRL-QB3-UCBerkeley/Denovotranscriptome>.

Finally, we used our annotated transcriptome to design capture probes to later sequence all coding regions (exome) from our target samples. We used this approach (a) because a full reference genome was not available a priori for these species, (b) to reduce the amount of sequencing necessary while still broadly sampling functionally

relevant genomic regions (exons and flanking sequences), and (c) to improve our ability to sequence low-quality and/or quantity DNA samples (i.e., old tissues and buccal swabs). Capture assays work well with low-quality/quantity DNA because the short probe lengths bind well to highly fragmented DNA and all off-target DNA is washed away before sequencing (Bi et al., 2013). To design our assay, we used a custom Nimblegen SeqCap EZ Developer Library (Roche Nimblegen Inc.). We tiled capture probes across the cds of each transcript and masked using both self and *Nanorana parkeri* genome frequency (max number of matches = 2). The resulting probe set covered 99.6% of the annotated transcripts for a total target size of 19.4 Mb from 24,863 targets.

2.4 | Sample library prep, capture, and sequencing

We selected a set of 186 historical, contemporary, and captive *A. varius* and *A. zeteki* samples to sequence using our exome capture targeted assay. We also sequenced four museum tissue samples from Costa Rican *Atelopus* specimens. Samples included multiple tissue types (toe clips, liver, tadpoles) and buccal swabs (see Table S1). Before DNA extraction, toe clips and tadpoles were stored in DESS buffer at room temperature, liver was stored in DMSO at -80°C , and buccal swabs were stored in 95% ethanol at -20°C . Liver, toes, and tadpoles were first rinsed with DNA-grade water and then homogenized using 2.8 mm ceramic beads and the MoBio PowerLyzer. Buccal swabs were dried at 37°C until all ethanol was evaporated. After initial sample prep, we followed the standard manufacturer's protocol for the Qiagen DNeasy Blood and Tissue kit with the addition of an RNase A treatment before adding Buffer AL and ethanol. Samples were eluted in 200 μl DNA-grade water and DNA concentration was measured using Qubit.

To prepare DNA samples for probe hybridization we used the KAPA Hyper Prep kit (Kapa Biosystems) for genomic library preparation. First, we sheared genomic DNA on a Diagenode Bioruptor to an average fragment size of 350 bp. We used 1.1 μg of DNA for sonication, unless the extraction yielded less than 1.1 μg , then the entire extraction was used (min = 24.5 ng, see Table S1). Sheared DNA was then cleaned using Kapa Pure Beads with a volumetric ratio of 1x. Cleaned DNA was prepped following the Kapa Hyper Prep protocol. Five microliters of 15 μM Illumina TruSeq Dual matched adapters was used in the ligation step. Samples were PCR amplified based on the initial amount of DNA (ranging from 2 to 12 cycles of amplification—see Table S1) with a target of 1 μg of DNA per sample post amplification. Post amplification, we performed a 0.6–0.8X double-sided size selection with Kapa Pure Beads. Samples were resuspended in 50 μl DNA-grade water. Sample quality was then assessed on an Agilent bioanalyzer and DNA concentration was measured using a Qubit. Equal amounts of DNA for each sample was then pooled into 12 pools, each with 16 samples.

Finally, to select only the targeted regions and wash away all other DNA fragments, we hybridized our DNA to capture probes. Target capture was performed following the Roche SeqCap EZ

Library SR protocol at the Functional Genomics Laboratory (FGL), a QB3-Berkeley Core Research Facility at UC Berkeley. At the FGL, the biotinylated probes were hybridized to 12 separate 1 μg pools, using SeqCap EZ Developer Reagent in place of COT1 Human DNA and universal blocking oligos provided by IDT (Xgen Universal Blockers-TS Mix), at 47°C for up to 72 hr. The hybridized samples were captured on streptavidin beads, and 14 cycles of post-capture PCR amplification was performed to enrich for target library fragments. Samples were then transferred to the Vincent J. Coates Genomic Sequencing Laboratory, a partner QB3-Berkeley Core Research Facility, quantified using Kapa Biosystems Universal Master Mix Illumina Quant qPCR reagents, pooled equimolar, and sequenced using four lanes of an Illumina HiSeq4000 paired-end 150 sequencing chemistry with dual 8-bp indexes. Sample data were then demultiplexed into fastq file format using Illumina bcl2fastq software version 2.19.

2.5 | Exome capture data processing

After sequencing, reads from all 190 samples were individually cleaned and aligned to prepare for downstream analyses. First, we processed the data using seqCapture (<https://github.com/CGRL-QB3-UCBerkeley/seqCapture>). We filtered raw reads using Trimmomatic (Bolger et al., 2014) and cutadapt (Martin, 2011) to trim adapter contaminations and low-quality reads. We removed exact PCR duplicates using Super-Deduper (<https://github.com/dstreeet/Super-Deduper>) and overlapping paired reads were merged using Flash (Magoč & Salzberg, 2011). We then selected eight representative libraries with the most amount of data and assembled each using Spades (Bankevich et al., 2012) with multiple kmer sizes (21, 33, 55, 77, 99, and 127). For each individual assembly, we used Blastn (Altschul et al., 1997) (evalue cutoff = $1\text{e}-20$, similarity cutoff = 80%) to compare the assembled contigs against the original annotated transcripts used for probe design and extracted the set of contigs associated with targets. We used Cd-hit-est (Li & Godzik, 2006) and Cap3 (Huang & Madan, 1999) to cluster and merge all raw assemblies into reduced, less-redundant assemblies. We then combined the assemblies for the eight individuals by a similar methodology. We generated a final exome reference sequence where all non-redundant and discrete contigs (exons and their flanking sequences) that were derived from the same target were joined with Ns based on their relative blast hit positions to the reference. We aligned cleaned sequence data from each individual library to this reference using Novoalign (<http://www.novocraft.com/products/novoalign/>) and only kept reads that mapped uniquely to the reference. We used Picard (<http://broadinstitute.github.io/picard/>) to add read groups and GATK v.3.8 (McKenna et al., 2010) to perform re-alignment. We then used SAMTools/bcftools (Li et al., 2009) to generate a raw variant call format (VCF) file that contains all potential variable and invariable sites. The VCF was then filtered using a custom filtering program, SNPcleaner (<https://github.com/tplinderoth/ngsQC/tree/master/snpCleaner>) by following the protocol specified in Bi et al. (2013). We only considered sites in which at least 70% of the

individuals had at least 3X coverage. We also filtered sites showing an excess of heterozygosity using a one-tailed exact test with a p -value of .00001. After these filters, 34.8 Mb sites from 14,985 genes (exons and flanking) were used in downstream population genetic analyses.

To check for signs of DNA damage between sample types, we used the program mapDamage2 (v.2.08; Jónsson et al., 2013). We assessed patterns of base misincorporations across sample types in raw reads in both the 3' and 5' direction.

2.6 | Population genetic structure analysis

First, to characterize variation and clustering in our ingroup samples ($N = 186$), we generated a PCA. With our low-medium coverage data, calling genotypes based only on allele counting (e.g., GATK) has high uncertainty (Nielsen et al., 2011); therefore, we called SNPs and estimated allele frequencies using an empirical Bayesian framework as implemented in ANGSD (v.0.919; Korneliussen et al., 2014). Using sites that passed the filters described above, we calculated genotype likelihoods using the SAMtools model (-GL 1) with an SNP p -value cutoff of 1×10^{-6} and formatted the output file using the -doGlf 2 flag. We then used pcangsd (v.0.9; Meisner & Albrechtsen, 2018) to generate a covariance matrix. We calculated eigenvalues and eigenvectors of the covariance matrix and plotted the first two eigenvectors in R (v.3.4.3). To compare genetic clustering patterns in populations with contemporary and historical samples, we repeated this process to create a PCA with only *A. varius* samples and for each individual population with contemporary individuals. Finally, to compare the relationship of Panamanian samples to samples from Costa Rica, we created a PCA with all samples sequenced in this study ($N = 190$).

To test for genetic clusters, we used NGSadmix as implemented in ANGSD (Skotte et al., 2013). First, we used ANGSD to calculate genotype likelihoods separately for all Panamanian samples ($N = 186$) and for all El Copé West samples ($N = 44$). For all samples, we ran NGSadmix for all values of K from 1 to 13, ten times, and for El Copé West we ran all values of K from 1 to 6, ten times. We then compared the likelihood values for each run using CLUMPAK (Kopelman et al., 2015) and calculated the most likely K using the ΔK method (Evanno et al., 2005).

To further understand the genetic relationship of individual samples, we calculated pairwise genetic distance using NGSdist v.1.0.2 (Vieira et al., 2016). First, we calculated genotype likelihoods for all samples ($N = 190$) using ANGSD -doGlf 8. We then calculated genetic distance using a subset of 1,422,762 sites. We repeated this calculation 100 times by randomly sampling with replacement blocks of 1,000 SNPs for bootstrap support values. We used FastME v.2.1.5 (Lefort et al., 2015) to calculate a neighbor-joining tree from the original distance matrix with bootstrap support values. We collapsed all nodes with <70 bootstrap support. To compare genetic distance to geographic distance we calculated pairwise geographic distance and plotted this versus genetic distance in R. We ran a Mantel test to assess statistical significance of the relationship between geographic and genetic distance. We also calculated a Mantel correlogram using

the Ecodist package (v.2.0.1) in R to compare the relationship of genetic and geographic distance across equally spaced geographic bins (Goslee & Urban, 2007).

To quantify genetic distinctiveness between populations, we calculated F_{ST} using ANGSD. First, we calculated the unfolded site frequency spectrum for each population separately and then calculated the joint site frequency spectrum for each comparison. We then calculated the global estimate for F_{ST} between populations in ANGSD using the "realSFS fst stats" function. We report the weighted F_{ST} value (Weir & Cockerham, 1984).

To test for, and to take into account the effect of isolation by distance on population clustering, we used clustering algorithm ConStruct that models both continuous and discrete population structure (Bradburd et al., 2018). To reduce computation times and even sampling among populations, we trimmed our sample set to a maximum of five individuals per sampling locality per time period (excluding El Copé West where we trimmed highly related individuals but allowed more than five individuals in the contemporary group). The final sample set included 117 individuals. We then randomly selected one SNP per contig for each of the samples ($N = 14,950$ SNPs) and ran construct in R (v.3.4.3) using spatial and nonspatial models for $K = 1$ to 5 with five replicates run for 10,000 iterations. We used the "x.validation" function in ConStruct to compare layer contributions and cross-validate the models.

2.7 | Genetic diversity and effective population size

To calculate within-population measures of genetic diversity, we first calculated the folded site frequency spectrum for populations as a whole and for individuals using ANGSD. We then calculated average heterozygosity, average per-site Watterson's theta (θ_W), and average per-site pi (π) for each population and time period using the filtered set of ~34 million sites (Korneliussen et al., 2013).

We calculated effective population size (N_e) using several methods. First, we used the program NeEstimator (v2.1) to calculate the N_e for each population using the linkage disequilibrium method (Do et al., 2014). We prepared an input file in Genepop format using a single randomly selected SNP per contig with no missing data ($N = 14,950$ SNPs) and excluded singleton alleles. We only report N_e for populations with at least 10 samples. Next, we used a sibship analysis as implemented in COLONY2 (Jones & Wang, 2010) to determine N_e of each subpopulation (across time and space). This analysis considers how many full and half sib dyads are present within a population to estimate the current effective size (Wang, 2009). To reduce computation time we selected a block of 2,000 SNPs, each from a separate contig, for each of the populations tested. We then ran COLONY2 using a polygamous mating system with inbreeding and a genotyping error rate of 0.0001. We used the full likelihood method with medium likelihood precision and medium run length. We did not specify male or female individuals a priori given these data are missing for many of our samples and we assumed random mating.

2.8 | Scans for selection

To reduce relatedness as a confounding factor, we trimmed highly related individuals from our dataset before performing our selection tests. To do this, we calculated pairwise relatedness between all in-group individuals using ngsRelate v.1 (Korneliussen & Moltke, 2015). To generate the input for ngsRelate, we first used ANGSD to call genotype likelihoods (GL -3) (Korneliussen et al., 2014). We then used ngsRelate to generate values for k_0 , k_1 , and k_2 . We calculated the coancestry coefficient (θ) between all individuals using the formula $\theta = k_1/4 + k_2/2$ where k_1 and k_2 are the maximum likelihood estimates of the relatedness coefficient (Jacquard, 1974). We then used these coancestry coefficients to trim our dataset for downstream selection analyses, removing one or more of a group of individuals that are highly related ($\theta > 0.25$ or putative siblings/parent-offspring). We trimmed seven individuals from the Santa Fe historical population and 13 individuals from the El Copé West contemporary population by randomly selecting one individual from each related group to remain in the sample set.

To search the *A. varius* exome for genetic variants that may be under selection in contemporary populations, we conducted three different time-stratified selection analyses across two different comparisons. Our comparisons include one broad analysis of shared signatures of selection across all *A. varius* (Historical: $N = 79$, Contemporary: $N = 26$) and one local comparison focused on the largest single contemporary population from El Copé West (Historical: $N = 14$, Contemporary: $N = 17$). Both datasets had close relatives removed as described above. The first analysis we used to identify putative genes under selection was an association test as implemented in ANGSD (-doasso 1). First, we coded historical individuals as control (0) and contemporary individuals as case (1). For each comparison, we calculated the likelihood ratio (LR) for each allele and compared these values to a chi-square distribution with $df = 1$ to get corresponding p -values. We also calculated per site F_{ST} and sliding window F_{ST} analyses to identify potential variants under selection. First, we calculated the unfolded site frequency spectrum for each trimmed population of interest using the reference fasta as the ancestral state. We then calculated the joint site frequency spectrum for each comparison and used the "realSFS" function in ANGSD to calculate the per site F_{ST} , and sliding window F_{ST} (window = 5,000 bp, step = 1,000 bp). Negative values for F_{ST} were treated as $F_{ST} = 0$. To assess the significance of outlier SNPs, we randomly permuted samples across historical/contemporary groups, breaking the phenotype-genotype connection. We then plotted this null distribution of F_{ST} values against the true F_{ST} values calculated for each comparison (Figure S3). This comparison tests the null hypothesis that $F_{ST} = 0$ for all SNPs; however, it does not distinguish between drift and selection as mechanisms driving $F_{ST} > 0$.

To evaluate the potential functional relevance of associated SNPs, we selected the top 50 associated SNPs from each method. We created a list of all unique contigs where these SNPs occurred for each comparison. To test for overrepresentation of shared biological functions within these lists, we used Blast2GO (v.5.2.5; Götz et al., 2008). First, we annotated the reference set of combined

genes and flanking regions using NCBI blastx and EMBL-EBI InterPro (Mitchell et al., 2014). We then used Blast2GO to run a Fisher's exact test for enrichment of specific biological processes, molecular functions, or cellular components in the set of candidate genes compared to the background set of all annotated genes ($N = 14,930$). We used an FDR filter at a significance level of 0.01.

3 | RESULTS

Our study presents the first genome-scale sequence dataset for the critically endangered *A. varius* and *A. zeteki* of Panamá. Our transcriptome-based capture array resulted in 34.8 million sites from 14,985 exons and flanking regions. Using our assay, we successfully sequenced genomic DNA from samples of varying DNA quality and/or quantity including minimally invasive buccal swabs, miniscule toe clips stored at room temperature for nearly two decades, and frozen museum tissues. Input DNA ranged from 25 to 1,577 ng (mean = 673 ng, Table S1). Our analysis found no difference in DNA damage patterns and a very low instance of base misincorporations across sample types (Figure S1), indicating that no biases were introduced due to differences in sample quality. Average coverage across filtered sites ranged from 5x to 31x (mean = 13x) for our samples.

Our sequence dataset includes a robust sample of *A. varius/zeteki* across time points (before and after *Bd* panzootic) throughout their range in Panama. We collected all contemporary samples from *A. varius* populations; we did not encounter *A. zeteki* during our contemporary surveys. While we collected contemporary samples from five distinct localities, a high percentage (77%, 30/39) of these came from a single locality—El Copé West. Furthermore, of the contemporary samples over half were juveniles (62%, 24/39), most of which were encountered at El Copé West in 2014. The prevalence of *Bd* in contemporary *A. varius* samples (25.6%, 10/39) matches the prevalence previously reported from the larger amphibian community in Panama (Voyles et al., 2018). *Bd* infection intensity across contemporary samples was highly variable, ranging from 25 to 1.4 million *Bd* DNA copies per swab (see Table S1). One adult (the only contemporary individual encountered at El Copé East) had an infection intensity similar to previously reported lethal pathogen loads for *A. zeteki* (DiRenzo et al., 2014). None of the contemporary individuals from the Caribbean were infected with *Bd* ($N = 5$).

3.1 | Population genetic structure

The genetic structure of *A. varius* and *A. zeteki* in Panamá indicates a pattern of isolation by distance (IBD; Figure S2). We found a significant linear relationship between geographic and genetic distance (Mantel $r = 0.599$, $p = .0001$; Figure S2A). Furthermore, the Mantel correlogram shows decreasing genetic relatedness over larger distances and reveals the tightest correlation between geographic and genetic distance between pairs within 20 km of each other (Figure S2B). The PCA of genetic variation clearly separates individual

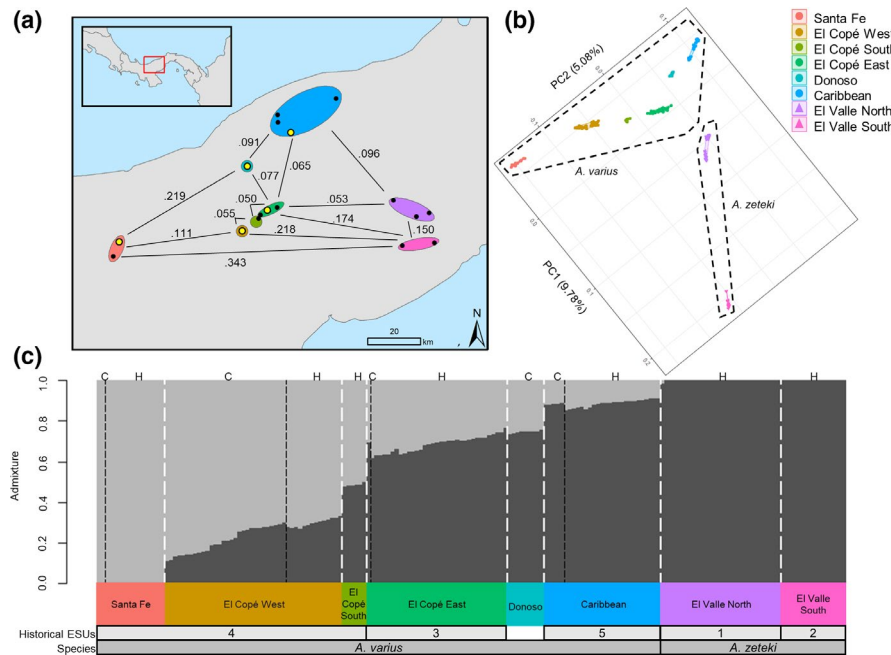


FIGURE 1 Geographic and genetic distribution of 186 *Atelopus varius* and *A. zeteki* samples showing a close match between sampling locality and location on genetic PC space. (a) Map of sampling localities with pairwise weighted F_{ST} values between adjacent populations. Individual sampling locations are marked with dots and populations indicated with colored ovals. Black dots indicate no contemporary surviving *A. varius/zeteki* and yellow dots indicate localities where contemporary *A. varius* were captured. (b) PCA from genetic covariance matrix. Samples separated into eight major clusters that correspond to geographic location of capture. Localities colored as in map. PCA is rotated to correspond to map of source populations. Historical species groups are labeled and marked with a dashed polygon. (c) Admixture plot for $K = 2$. White dashed lines separate localities and black dashed lines within localities separate contemporary (left) and historical (right) individuals. Evolutionarily significant units (ESUs) and species designations from Richards and Knowles (2007) are listed below sampling localities

populations into their respective sampling localities (Figure 1a,b). Based on the PCA and original sampling locality, we grouped *Atelopus* into eight distinct genetic groups. Of these eight groups, six were historically described as *A. varius* populations and two were described as *A. zeteki*. We found that average pairwise weighted F_{ST} between the two populations of *A. zeteki* was greater than the F_{ST} between some populations of *A. varius* and *A. zeteki* (Figure 1a). Furthermore, our admixture plot showing $K = 2$ (best K as determined using the ΔK method, Evanno et al., 2005) indicates that each genetic cluster is not restricted to either of the two species (Figure 1c). Rather, there is a gradual change in admixture proportions as you go from East to West, with *A. zeteki* representing one genotype and the Santa Fe population of *A. varius* representing the other extreme. All other *A. varius/zeteki* samples show admixture from both groups (Figure 1c).

To account for the effect of IBD in our cluster analysis, we ran conStruct, which explicitly models genetic covariance across space while calculating admixture proportions (Bradburd et al., 2018). This method considers different “layers” from which an individual can draw admixture from. First, by looking at the relative contributions of additional layers, we found that layers beyond $K = 2$ contributed little admixture to each sample (Figure S3B). Furthermore, we found that the spatial model had higher predictive power across all values of K from 1 to 5 (Figure S3A). These findings indicate that IBD is strong in the dataset and that $K = 2$ best explains our data. By comparing

the spatial and non-spatial structure plots (Figure S3C), we see that at $K = 2$ admixture patterns between spatial and non-spatial models are similar. Furthermore, at higher values of K for both spatial and non-spatial models, there are rarely instances of clear population level separation or structuring in this dataset.

3.2 | Genetic diversity and N_e

Genetic diversity and heterozygosity are variable within each historical population. The least genetically diverse population is *A. zeteki* from El Valle South. This population had the highest average relatedness (Figure 2a) and lowest heterozygosity (Figure 2b). The next highest average relatedness is in the Santa Fe population of *A. varius* (Figure 2). These two populations represent the extremes of the sampled range for this study (Figure 1a). In general, there is a pattern of decreasing heterozygosity as you move from West to East for these species (Figure 2b), revealing that heterozygosity was quite low for the putatively extinct in the wild *A. zeteki*.

We found a marked decrease in genetic diversity in the group of all contemporary *A. varius* compared to historical *A. varius* (Table 1). There was a 27% decrease in θ_{wv} , and a 3% decrease in π over this time period. This pattern holds true when considering the individual cases of El Copé West ($\Delta\theta_{wv} = -14\%$, $\Delta\pi = -12\%$), Caribbean

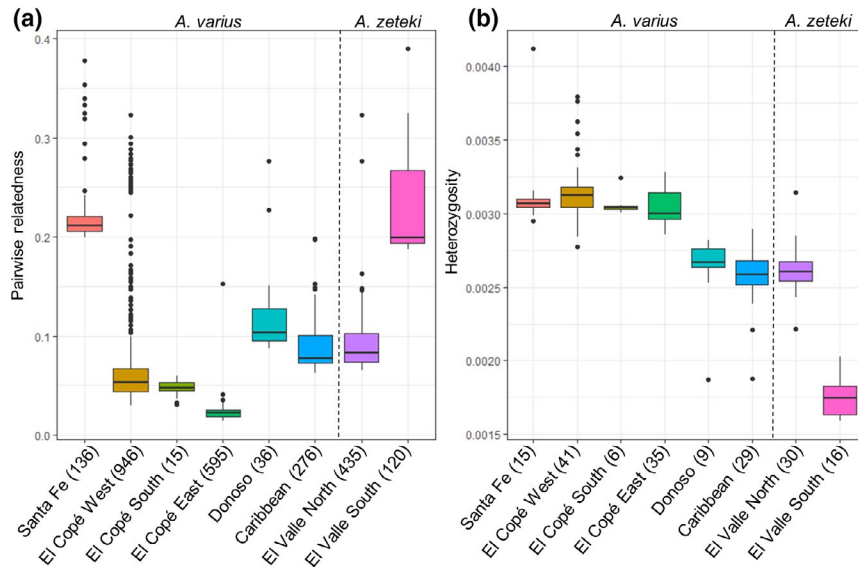


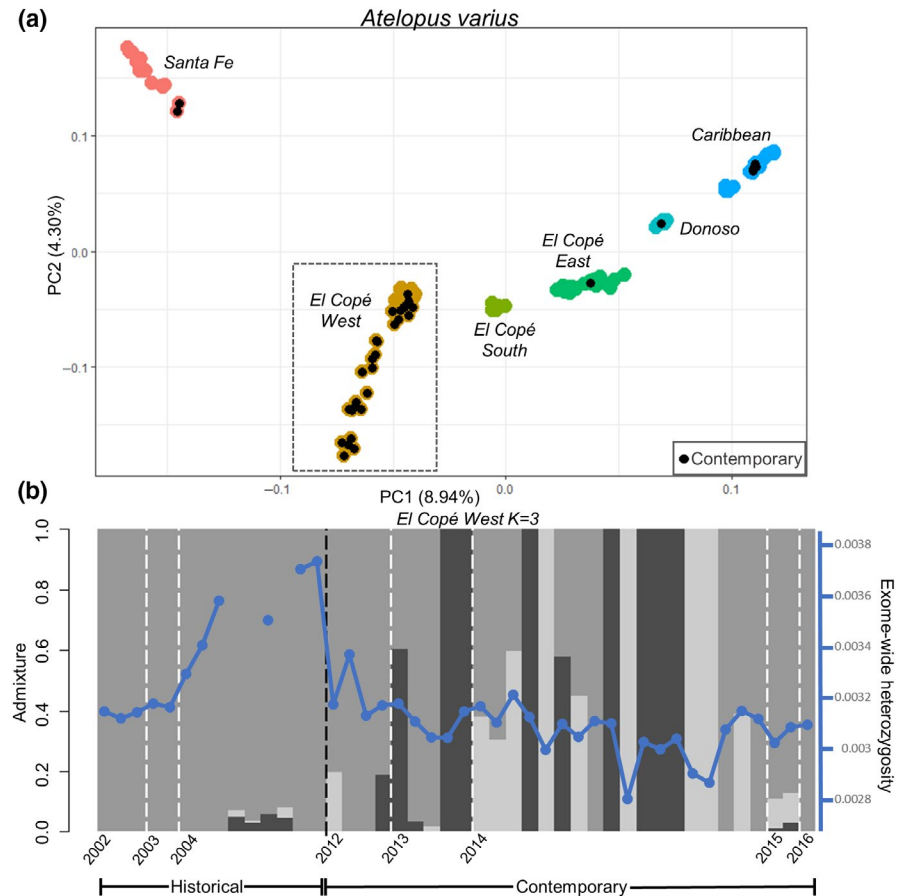
FIGURE 2 Boxplots showing high pairwise relatedness at the eastern and western-most localities and a decrease in heterozygosity from west to east. Species names are shown above, and number of pairwise comparisons (a) or number of individuals (b) are indicated in parentheses after population labels. Populations colored as in Figure 1. (a) Pairwise relatedness within each population, as measured using the coancestry coefficient (θ). (b) Exome wide heterozygosity for individuals from each population

TABLE 1 Average per-site Watterson's theta (θ_w), average per-site pi (π), and average heterozygosity for samples grouped by species and population. All are calculated using the folded site frequency spectrum. Average pairwise relatedness is calculated from relatedness coefficients using ngsRelate. Ne are calculated in two different ways (a) using the LD method as implemented in NeEstimator (v2.1)–95% CI are from Jackknifing across samples and (b) using a sibship analysis implemented in COLONY

Population	θ_w	π	Ne – NeEstimator (LD) [95% CI]	Ne – COLONY (SA) [95% CI]	Average heterozygosity	Average relatedness	N
<i>A. varius</i> historical	0.0062	0.0032	69 [54,93]	121 [89,166]	0.0031	0.0215 ^a	86
<i>A. varius</i> contemp.	0.0045	0.0031	36 [24,61]	41 [27,68]	0.0030	0.0490 ^a	39
<i>A. zeteki</i> historical	0.0032	0.0025	43 [30,67]	54 [35,87]	0.0023	0.0894	44
El Copé West (<i>A. varius</i>)							
Historical	0.0043	0.0034	266 [113,inf]	[1,inf]	0.0037 ^a	0.0610 ^a	14
Contemporary	0.0037	0.0030	26 [16,50]	36 [22,65]	0.0031 ^a	0.0730 ^a	30
Santa Fe (<i>A. varius</i>)							
Historical	0.0037	0.0030	15 [8,41]	38 [20,97]	0.0033	0.2227	15
Contemporary	0.0030	0.0029			0.0030	0.2040	2
El Copé South (<i>A. varius</i>)							
Historical	0.0034	0.0030			0.0031	0.0472	6
El Copé East (<i>A. varius</i>)							
Historical	0.0045	0.0030	1,650 [875,13559]	[1,inf]	0.0031	0.0213	27
Captive	0.0034	0.0029			0.0030	0.0276	7
Donoso (<i>A. varius</i>)							
Captive	0.0027	0.0026			0.0027	0.1179	8
Caribbean (<i>A. varius</i>)							
Historical	0.0029	0.0026	136 [98,218]	552 [209,inf]	0.0026	0.0878 ^a	24
Contemporary	0.0025	0.0025			0.0025	0.1066 ^a	5
El Valle North (<i>A. zeteki</i>)							
Historical	0.0032	0.0026	164 [94,559]	378 [176,inf]	0.0026	0.0876	28
Captive	0.0025	0.0025			0.0026	0.0939	2
El Valle South (<i>A. zeteki</i>)							
Historical	0.0016	0.0018	13 [9,18]	44 [21,136]	0.0017	0.2310	16

^aIndicates significant difference between historical and contemporary samples for heterozygosity and average relatedness (Mann–Whitney U test $p < .01$).

FIGURE 3 PCA and admixture plots of *Atelopus varius* samples reveal a unique genetic pattern at El Copé West. (a) PCA from genetic covariance matrix of historical (color only) and contemporary (black center) *A. varius* samples. (b) Admixture plot for all El Copé West samples showing the best $K = 3$. Samples are sorted based on date of collection and historical and contemporary samples are separated by a black dashed line. Exome-wide heterozygosity for each individual is shown in the blue dot plot. Additional visualizations for El Copé West can be seen in Figure S7)



($\Delta\theta_W = -14\%$, $\Delta\pi = -4\%$), and Santa Fe ($\Delta\theta_W = -19\%$, $\Delta\pi = -3\%$). Genetic diversity is also lower in the captive populations of *A. zeteki*/*varius* as compared to their original source populations (Table 1). The small difference in heterozygosity between all contemporary and historical *A. varius* was not significant (Mann-Whitney U test $p = .58$). However, there was a significant decrease in heterozygosity in El Copé West in contemporary versus historical samples ($\Delta H_e = -16\%$, Mann-Whitney U test $p < .0001$, Figure 3b).

Effective population size is low for all contemporary populations. Considering all *A. varius*, N_e decreased by 48% from the historical to the contemporary time period based on the LD analysis (N_e historical = 69, N_e contemporary = 36). The sibship analysis estimated a more severe decrease of 66%. Historically, El Copé East had the highest N_e of 1,650. All other historical populations had very low N_e , especially the inbred populations of *A. zeteki* in El Valle South ($N_e = 13$) and *A. varius* from Santa Fe ($N_e = 15$).

3.3 | Local patterns of genetic diversity and structure

Our data reveal that the single locality with the most contemporary samples, El Copé West, has a unique genetic relationship between the historical and contemporary individuals (Figure 3; Figure S4). All contemporary samples sequenced from other localities are genetically

indistinguishable from the historical population sampled at that locality (Figure 3a; Figure S4). In contrast, at El Copé West, contemporary individuals are much more genetically variable than their historical counterparts (Figure 3a; Figure S4). Based on the NGSadmix and CLUMPAK analysis, we found that the most likely $K = 3$ for this population. From the admixture analysis, we see that the contemporary samples include three distinct genetic clusters, two of which are minimally represented in the historical sample set (Figure 3b; Figure S5). Contemporary individuals from El Copé West also show more admixture than those from the historical group. Seven samples from the contemporary group show at least 25% admixture from two different genetic groups, while none of the historical samples do. Additionally, within the contemporary samples from El Copé West, we found evidence of successful breeding and maturation to ~6 months for at least two separate clutches (based on relatedness analysis). However, none of the 19 juveniles found in 2014 were encountered again in subsequent surveys. Overall, the contemporary samples from El Copé West revealed a unique genetic relationship to historical samples from the same locality, a pattern which was not found at other localities with contemporary individuals.

3.4 | Tests for survival-associated genes

With the goal of generating a list of potential candidate genes for future studies, we leveraged our paired time series data to look

TABLE 2 Outlier contigs and associated annotations for global *Atelopus varius* analysis. List of 61 genes that contain associated SNPs for contemporary *A. varius*

Contig name	Annotation	Outlier detection method	N SNPs	N F_{ST} windows	Allele frequency change
combined_Contig473	TPA: putative transposase	Fstwin	0	1	NA
combined_Contig708	Cytochrome P450 2K1	asso, Fst	1	0	0.17
combined_Contig726	Probable alpha-ketoglutarate-dependent hypophosphite dioxxygenase	Fst	1	0	0.19
combined_Contig963	Adenylosuccinate synthetase isozyme 2	asso, Fstwin	1	2	0.44
combined_Contig1050	Toll-like receptor 1 (TLR1)	Fst	1	0	0.19
combined_Contig1123	Solute carrier family 2, facilitated glucose transporter member 11-like	Fst	1	0	0.32
combined_Contig1242	Protein-lysine methyltransferase METTL21D	asso	1	0	0.20
combined_Contig1363	Poly [ADP-ribose] polymerase 4-like	asso	1	0	0.40
combined_Contig1472	Olfactory receptor 6N2-like	asso	1	0	0.40
combined_Contig1601	Protein unc-93 homolog A-like	asso, Fst	2	0	0.42–0.43
combined_Contig2446	Protein spinster homolog 1-like	asso	1	0	0.41
combined_Contig3340	VPS10 domain-containing receptor SorCS2	Fst	1	0	0.20
combined_Contig3424	Replication protein A 14 kDa subunit	asso, Fst	1	0	0.43
combined_Contig3518	Interferon-induced 35 kDa protein	asso, Fst	1	0	0.25
combined_Contig3827	Neuropeptide Y receptor type 1-like	Fst	1	0	0.25
combined_Contig4454	Sodium/potassium/calcium exchanger 2 isoform X1	asso	1	0	0.40
combined_Contig4938	Ribonuclease T2 L homeolog isoform X1	Fstwin	0	1	NA
combined_Contig4941	Kynurenine 3-monooxygenase	Fstwin	0	3	NA
combined_Contig4943	Lysosomal-trafficking regulator (LYST)	asso, Fstwin	5	19	0.40–0.45
combined_Contig5063 ^a	Transmembrane protein 131-like (TMEM131)^a	asso, Fst	1	0	0.21
combined_Contig5390	Coiled-coil domain-containing protein 22	Fst	1	0	0.19
combined_Contig5608 ^a	Zinc finger protein 518B-like (ZNF518B) ^a	asso, Fst	1	0	0.35
combined_Contig5975	Centrosomal protein of 170 kDa-like isoform X1	asso	1	0	0.43
combined_Contig6021 ^a	Lysine-specific histone demethylase 1B isoform X1 (KDM1B) ^a	asso, Fst	1	0	0.42
combined_Contig6469	Zinc finger protein 638	asso, Fst	1	0	0.26
combined_Contig6941	PREDICTED: uncharacterized protein LOC108790942	asso, Fstwin	1	1	0.40
combined_Contig6942	Nuclear pore complex protein Nup133	asso, Fstwin	1	4	0.45
combined_Contig7024	T-lymphoma invasion and metastasis-inducing protein 1 isoform X1	asso, Fst	2	0	0.36–0.37
combined_Contig7123	Titin-like isoform X32	asso, Fst	5	0	0.30–0.31
combined_Contig7251	LOC548985 protein	asso	2	0	0.30
combined_Contig7495	Protein disulfide-isomerase-like protein of the testis	Fst	1	0	0.30
combined_Contig7505	Promethin-A isoform X1	Fst	1	0	0.23
combined_Contig7677	Interferon-induced transmembrane protein 3-like	Fst	1	0	0.32
combined_Contig8245	Neuron navigator 1	Fst	1	0	0.40

(Continues)

TABLE 2 (Continued)

Contig name	Annotation	Outlier detection method	N SNPs	N F_{ST} windows	Allele frequency change
combined_Contig8274	A disintegrin and metalloproteinase with thrombospondin motifs 13 (ADAMTS13)	Fst	1	0	0.28
combined_Contig8333	Histone chaperone ASF1A	asso, Fst	3	0	0.32–0.35
combined_Contig8554	General transcription factor 3C polypeptide 5	asso, Fst	1	0	0.28
combined_Contig8659	Carnitine o-palmitoyltransferase muscle isoform isoform 1	asso, Fst	1	0	0.18
combined_Contig9310	Spectrin alpha chain, non-erythrocytic 1	asso	1	0	0.40
combined_Contig9344	Transmembrane protein 223 isoform X1	Fst	1	0	0.25
combined_Contig9477	Misshapen-like kinase 1 isoform X2	asso, Fst	1	0	0.26
combined_Contig9605	Phosphofurin acidic cluster sorting protein 1-like	Fst	1	0	0.30
combined_Contig9813	Myotubularin-related protein 6	Fst	1	0	0.22
combined_Contig10055 ^a	bis(5'-adenosyl)-triphosphatase (ENPP4)^a	asso, Fst	1	0	0.34
combined_Contig10067	Aminoacyl tRNA synthase complex-interacting multifunctional protein 2 isoform X2	asso	1	0	0.19
combined_Contig10096	Eyes absent homolog 3	asso, Fst	1	0	0.30
combined_Contig11387	Golgin subfamily B member 1-like	Fst	1	0	0.25
combined_Contig12499	Transformation/transcription domain-associated protein	asso, Fst	1	0	0.21
combined_Contig12753	Meteorin-like protein	asso	1	0	0.42
combined_Contig13296	Protein arginine methyltransferase NDUFAF7, mitochondrial precursor	Fstwin	0	1	NA
combined_Contig13379	Fumarate hydratase, mitochondrial	Fstwin	0	1	NA
combined_Contig13502	CCAAT/enhancer-binding protein zeta	asso, Fst, Fstwin	2	4	0.40–0.48
combined_Contig13521	TPA: putative transposase	asso, Fst, Fstwin	2	5	0.41–0.42
combined_Contig13561	TAF5-like RNA polymerase II p300/CBP-associated factor-associated factor 65 kDa subunit 5L	Fstwin	0	1	NA
combined_Contig13570	Conserved oligomeric Golgi complex subunit 2	Fstwin	0	5	NA
combined_Contig13631	Cytochrome c oxidase subunit 5B, mitochondrial-like	Fst	3	0	0.18–0.27
combined_Contig13777 ^a	Transcription cofactor vestigial-like protein 4 (VGLL4) ^a	Fst	1	0	0.31
combined_Contig13778	Methenyltetrahydrofolate synthase domain-containing protein	Fst	1	0	0.28
combined_Contig14222	Exocyst complex component 8	Fstwin	0	1	NA
combined_Contig14696	Probable cytosolic iron-sulfur protein assembly protein ciao1	asso, Fst	2	0	0.24
combined_Contig15194	Proteasome subunit beta type-2	Fst	1	0	0.32

^aIndicates contigs shared across El Copé West and *A. varius* analyses. Bold genes are discussed in the main text.

for SNPs associated with persisting individuals in this system. By combining candidate SNPs from genes discovered via association test, F_{ST} outlier test, and F_{ST} sliding window analysis, we created a list of 61 unique genes for the comparison of all historical and contemporary *A. varius* (Table 2) and 76 unique genes for the comparison of historical and contemporary individuals from El Copé West

(Table 3). Here, unique genes are defined as the contig containing the outlier SNP or SNPs from our assembled reference. Allele frequency changes between contemporary and historical populations for the list of 61 genes in the *A. varius* comparison ranged from 17% to 45%. For the 76 outlier genes in the El Copé West, comparison allele frequency changes ranged from 38% to 58%. While this list

TABLE 3 Outlier contigs and associated annotations for local El Copé West analysis. List of 76 genes that contain associated SNPs for contemporary *Atelopus varius* at El Copé West

Contig name	Annotation	Outlier detection method	N SNPs	N F_{ST} Windows	Allele frequency change
combined_Contig212	Zinc finger protein 180 isoform X1	Fstwin	0	1	NA
combined_Contig1205	LOC100127334 protein	Fstwin	0	1	NA
combined_Contig1263	Solute carrier family 22 member 7-like	Fstwin	0	1	NA
combined_Contig1417	Uncharacterized methyltransferase-like C25B8.10	asso	1	0	0.33
combined_Contig2428	mdm2-binding protein	asso	1	0	0.32
combined_Contig2601	Ethanolamine-phosphate cytidylyltransferase isoform X1	asso, Fst, Fstwin	1	1	0.39
combined_Contig2972	Capn1 protein	Fst, Fstwin	1	1	0.50
combined_Contig3007	Oncostatin-M-specific receptor subunit beta	asso	1	0	0.37
combined_Contig3643	Hermansky-Pudlak syndrome 5 protein-like	asso, Fst	1	0	0.32
combined_Contig3740	Phosphatidylinositol 4-phosphate 5-kinase type-1 beta isoform X2	asso	1	0	0.36
combined_Contig5063 ^a	Transmembrane protein 131-like (TMEM131)^a	asso, Fst	2	0	0.35–0.43
combined_Contig5369	Serine/threonine-protein phosphatase 4 regulatory subunit 3	Fstwin	0	1	NA
combined_Contig5608 ^a	Zinc finger protein 518B-like (ZNF518B) ^a	Fstwin	0	1	NA
combined_Contig5933	Probable global transcription activator SNF2L2 isoform X1	Fst, Fstwin	1	3	0.49
combined_Contig5977	Adipocyte plasma membrane-associated protein-like	asso	1	0	0.39
combined_Contig6001	Collagen alpha-1(XX) chain	asso, Fst	1	0	0.46
combined_Contig6019	Nuclear pore complex protein Nup153	asso, Fst, Fstwin	1	8	0.52
combined_Contig6021 ^a	Lysine-specific histone demethylase 1B isoform X1 (KDM1B) ^a	asso, Fst	1	0	0.58
combined_Contig6146	Mitochondrial ribosome-associated GTPase 2 isoform X1	Fst	1	0	0.44
combined_Contig6151	U4/U6 small nuclear ribonucleoprotein Prp3	asso, Fst, Fstwin	1	1	0.42
combined_Contig6295	Laminin subunit alpha-5	asso, Fst	7	0	0.38–0.48
combined_Contig6623	Xemd1 protein	Fstwin	0	1	NA
combined_Contig6773	Mitogen-activated protein kinase 4	Fst	1	0	0.43
combined_Contig7200	MGC78973 protein	Fst	1	0	0.48
combined_Contig7281	Transmembrane and coiled-coil domain-containing protein 6-like	Fstwin	0	1	NA
combined_Contig7713	Gastrula zinc finger protein XICGF17.1-like	Fstwin	0	1	NA
combined_Contig8034	Lipoyltransferase 1, mitochondrial	Fstwin	0	1	NA
combined_Contig8734	disco-interacting protein 2 homolog B	asso, Fst	1	0	0.42
combined_Contig8998	LOC733236 protein	asso, Fst	1	0	0.57
combined_Contig9237	E3 ubiquitin-protein ligase MYCBP2	Fstwin	0	2	NA
combined_Contig9468	striatin-interacting protein 2 isoform X2	asso	1	0	0.33
combined_Contig9792	hsp70-binding protein 1	asso, Fst	1	0	0.36
combined_Contig10016	PREDICTED: uncharacterized protein C18orf8 homolog	asso	1	0	0.39

(Continues)

TABLE 3 (Continued)

Contig name	Annotation	Outlier detection method	N SNPs	N F_{ST} Windows	Allele frequency change
combined_Contig10055 ^a	bis(5'-adenosyl)-triphosphatase (ENPP4) ^a	asso, Fstwin	1	1	0.33
combined_Contig10520	Ectonucleotide pyrophosphatase/ phosphodiesterase family member 1 ENPP1	asso, Fst	1	0	0.51
combined_Contig10543	NXPE family member 4-like	asso, Fst	1	0	0.32
combined_Contig10696	charged multivesicular body protein 4b	asso	1	0	0.32
combined_Contig10697	AN1-type zinc finger protein 1 [<i>Xenopus tropicalis</i>]	asso, Fst	1	0	0.44
combined_Contig10810	Unconventional myosin-IXb	asso, Fst, Fstwin	2	9	0.41–0.49
combined_Contig10900	Monocarboxylate transporter 14	Fst	1	0	0.47
combined_Contig10917	Cytochrome c oxidase assembly protein COX11, mitochondrial	asso, Fst	2	0	0.35–0.39
combined_Contig11234	cbp/p300-interacting transactivator 2	Fstwin	0	1	NA
combined_Contig11237	Transmembrane protein 132A-like	asso	1	0	0.33
combined_Contig11288	Toll-like receptor 4 (TLR4)	asso, Fst	1	0	0.32
combined_Contig11457	RNA demethylase ALKBH5	asso, Fst	1	0	0.43
combined_Contig11459	Mitochondrial dynamics protein MID49	Fst	1	0	0.45
combined_Contig11470	Fumarylacetoacetate hydrolase domain- containing protein 2 isoform X1 (FAHD2)	asso, Fst, Fstwin	4	1	0.41–0.47
combined_Contig11552	Calpain-3 isoform X6	Fstwin	0	1	NA
combined_Contig11606	Serine/threonine protein kinase	asso, Fst	1	0	0.32
combined_Contig11652	Novel Trtraspanin family protein	Fst	1	0	0.46
combined_Contig11762	Phosphoglucosyltransferase-like protein 5	asso, Fst	1	0	0.32
combined_Contig12056	A disintegrin and metalloproteinase with thrombospondin motifs 3	asso	2	0	0.36–0.39
combined_Contig12085	TPA: putative transposase	Fst	1	0	0.38
combined_Contig12325	DAZ associated protein 2	Fstwin	0	1	NA
combined_Contig12326	Small transmembrane and glycosylated protein homolog	Fstwin	0	1	NA
combined_Contig12730	Transmembrane protein 205 isoform X1	asso, Fst	1	0	0.42
combined_Contig12815	Regulator of nonsense transcripts 3B isoform X1	Fst, Fstwin	1	1	0.36
combined_Contig13139	Integrin alpha-6 isoform X3	asso	1	0	0.33
combined_Contig13170	Sortilin 1 S homeolog precursor	asso	1	0	0.35
combined_Contig13349	Coiled-coil domain-containing protein 39	Fstwin	0	2	NA
combined_Contig13370	Alpha-2-macroglobulin-like protein 1	asso	1	0	0.34
combined_Contig13456	Protein Jade-3	Fstwin	0	1	NA
combined_Contig13463	Attractin-like protein 1	asso, Fst	1	0	0.46
combined_Contig13467	Calcium uniporter regulatory subunit MCUB, mitochondrial-like	Fstwin	0	1	NA
combined_Contig13491	RING finger protein 121	asso, Fst	1	0	0.43
combined_Contig13532	Cytoplasmic polyadenylation element- binding protein 4 isoform X1	asso	1	0	NA
combined_Contig13694	ELAV-like protein 1	Fstwin	0	1	NA
combined_Contig13776	Properdin factor, complement	asso	1	0	0.52
combined_Contig13777 ^a	Transcription cofactor vestigial-like protein 4 (VGLL4) ^a	Fstwin	0	1	NA

(Continues)

TABLE 3 (Continued)

Contig name	Annotation	Outlier detection method	N SNPs	N F_{ST} Windows	Allele frequency change
combined_Contig14016	Islet cell autoantigen 1 isoform X1	asso, Fst	1	0	0.46
combined_Contig14195	LOC100037234 protein	Fstwin	0	1	NA
combined_Contig14434	Eukaryotic translation initiation factor 4 gamma 1 isoform X1	Fst	2	0	0.46
combined_Contig14586	ADP-ribosyltransferase 5	Fstwin	0	1	NA
combined_Contig14622	Solute carrier family 12 member 8 isoform X1	Fstwin	0	1	NA
combined_Contig14943	Laminin subunit beta-1-like	asso	1	0	0.33
combined_Contig15350	C4SR protein	Fst	1	0	0.40

^aIndicates contigs shared across El Copé West and *A. varius* analyses. Bold genes are discussed in the main text.

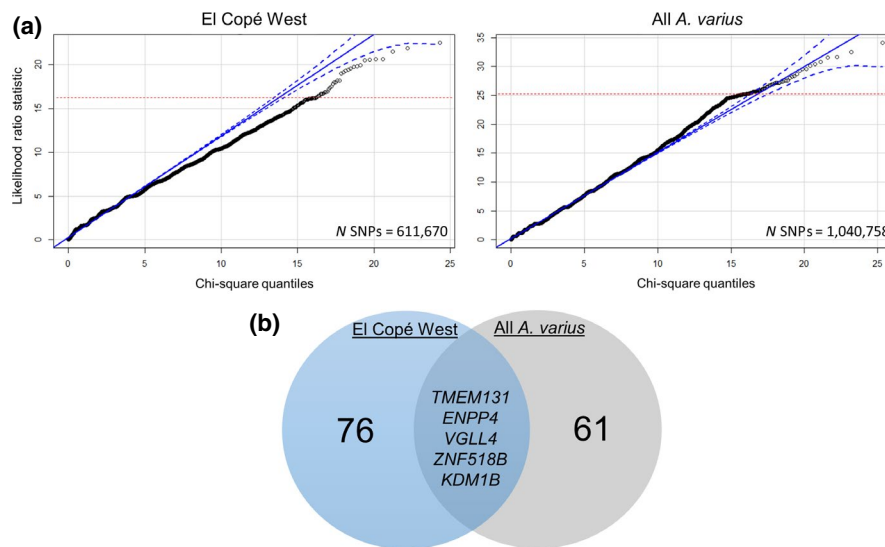


FIGURE 4 (a) Quantile–quantile plots for El Copé West (left) and all *Atelopus varius* (right). Points are the likelihood ratio statistic for every SNP calculated by ANGSD -doAsso 1 and are chi-squared distributed with $df = 1$. Blue lines represent a robust regression line with a 95% confidence interval as implemented in the qqPlot function in the car package (v.3.0.2) in R (v.3.4.3). Red dashed line indicates the value above which lie the top 50 most highly associated SNPs (El Copé West: LRT = 16.00, FDR $p = .95$; *A. varius*: LRT = 25.49, FDR $p = .007$). (b) Number of candidate genes for each comparison after combining list of top 50 genes from association test, F_{ST} outlier test, and F_{ST} sliding window test. Five shared genes found in both the global and local comparison are listed

was created from highly associated SNPs, none are statistically significant after correcting for multiple tests—see qqPlots showing results from association tests (Figure 4a) and plots of per-site F_{ST} versus permutation-generated null F_{ST} distributions (Figure S6). We compared these lists to find overlap between the El Copé West and *A. varius* comparisons (Figure 4b) and found five genes included in both lists. We found no enrichment for specific biological processes, molecular functions, or cellular components in the set of combined genes or any of the separate candidate gene lists after using a Fisher's exact test with FDR correction for multiple tests ($\alpha = 0.05$). We manually identified potential candidate genes in each list that may be related to *Bd*-specific biological processes. We present these in Tables 2 and 3 and discuss their functions further below.

Although we did not find strong evidence for selection on particular genetic pathways, our data provide important candidate

loci for continued study. Beginning with the local comparison in El Copé West (Table 3), we identified several associated SNPs in immune-related genes—one SNP in a toll-like receptor 4 (TLR4) gene and another in a gene for a properdin factor in the complement system. Two genes with the strongest signal of association in this comparison were laminin subunit alpha-5 (seven associated SNPs) and fumarylacetoacetate hydrolase domain-containing protein 2 (FAHD2, four associated SNPs). In the larger *A. varius* comparison (that included all contemporary and historical *A. varius* populations), we found several highly associated SNPs in genes of interest (Table 2). First, we found another associated SNP in a toll-like receptor gene (TLR1). Additionally, one gene that had a very strong signal of association (5 highly associated SNPs and 19 outlier F_{ST} sliding windows for a total of 28,000 bp) was a lysosomal-trafficking regulator gene (LYST). We also document a highly

associated SNP in an interferon-induced 35 kDa protein. Finally, two SNPs in a T-lymphoma invasion and metastasis-inducing protein 1 gene were also present in our list of associated SNPs for the *A. varius* comparison. Five genes had outlier SNPs in both the local El Copé West analysis and the larger comparison of all *A. varius* (Figure 4): transmembrane protein 131 (TMEM131), bis(5'-adenosyl)-triphosphatase (ENPP4), transcription cofactor vestigial-like protein 4 (VGLL4), zinc finger protein 518B (ZNF518B), and lysine-specific histone demethylase 1B (KDM1B). Below we discuss these genes in more detail and relate our findings to previous studies on molecular mechanisms of *Bd* resistance in amphibians.

4 | DISCUSSION

By comparing historical and contemporary genome-wide variation in two endangered *Atelopus* species, we document sharp and dramatic decreases in genetic diversity and effective population size following *Bd*-related declines. Moreover, we identify demographic and adaptive processes that may contribute to persistence. Overall, our genetic data can serve to inform conservation decisions for natural and captive populations of these ecologically and culturally important species. Additionally, we investigate genetic mechanisms of persistence after rapid population declines and identify specific genetic variants associated with *Atelopus* persistence that can spur future research and conservation efforts.

4.1 | Identifying relevant conservation units

Atelopus varius and *A. zeteki* have traditionally been separated into two species and managed as five distinct evolutionarily significant units (ESUs; Richards & Knowles, 2007; Zippel et al., 2006). These ESUs also inform how these species are managed in captivity—frogs are only bred within their designated ESU (Estrada et al., 2014). However, the genetic analysis used to support the ESU designations was limited to two mitochondrial markers, which alone were not sufficient to delineate the ESUs. The ESUs were delineated based on both genetic and phenotypic data (Richards & Knowles, 2007), although phenotypes for these species are highly variable across short geographic distances (Savage, 1972). Another recent study using two mitochondrial genes supports the current *A. varius/zeteki* split but reports little statistical support for internal nodes and overlapping ranges for these species (Ramírez et al., 2020). Therefore, our genome-wide dataset can serve to clarify the relationships among populations of these species. Many of the historical samples sequenced in both mitochondrial DNA-based studies (Ramírez et al., 2020; Richards & Knowles, 2007) were re-sequenced for this study, giving us high power to test the original ESU/species boundary hypotheses.

Our data do not support the delineation of *A. varius* and *A. zeteki* into five distinct ESUs and calls into question the original species boundary. We show that the distance between source populations

is highly correlated with genetic distance. Rather than distinct genetic breaks between populations, these species show a continuous increase in genetic distance with increasing geographic distance (Figure S2). To account for IBD in our genetic cluster analysis, we ran the program conStruct, which explicitly accounts for the decay in relatedness between samples due to distance (Bradburd et al., 2018). Our conStruct results show that for both spatial and non-spatial models from $K = 2$ to $K = 5$, there are few instances of clearly defined genetic layers that are exclusive to a certain population or group of populations (Figure S3). Most historical ESUs correspond to specific populations identified in our PCA analysis (ESUs 1, 2, 3, 5). However, other ESUs group genetically distinct populations together (ESU 4). In our study, we see that individuals on the extremes of the range (i.e., *A. zeteki* from El Valle and *A. varius* from Santa Fe) are genetically distinct from one another, but all other populations show a pattern of isolation by distance. Drawing species boundaries in the case of continuous genetic differentiation is a common and long-standing challenge in conservation (Moritz, 1994) and further work that puts the variation in Panamanian harlequin frogs in a broader geographic and taxonomic context is needed.

For now, our data indicate that *A. varius* and *A. zeteki* from central Panamá may be best managed according to their source population, as most individuals from a single locality cluster closely with other individuals captured at that locality (Figure 2a). Genetic clustering based on geography, and management as such, aligns with the natural history of these species—*A. varius* exhibit high site fidelity (Crump, 1986). However, limitations in the genetic diversity of captive populations may mean that animals need to be bred across populations. Given the high levels of admixture between most nearby populations in the wild, we suggest that geographic proximity be considered a good proxy for relatedness in this species. Breeding across populations that are geographically and genetically proximate, even if they are currently considered different species, may be necessary. For example, we found that the two populations of *A. zeteki* (El Valle North and El Valle South) are more diverged from each other than the El Valle North population is from El Copé East *A. varius* (Figure 1). Furthermore, the current captive population of *A. zeteki* in Panamá was collected from El Valle North and there are only four founders currently alive or represented in this collection (Panama Amphibian Rescue & Conservation Project, 2019). Therefore, integrating new understandings of the genetic relationships between populations of these species will be critical for captive management going forward.

Furthermore, our findings from the distance-based phylogenetic analyses and PCA that include Costa Rican samples support our conclusions that geographic distance is the best predictor of *Atelopus* genetic relatedness and indicate some taxonomic confusion for the *Atelopus* of western Panamá and Costa Rica. We found that geographic distance was a better predictor of genetic distance, not only for our focal species, but also for the four Costa Rican samples. For example, one *A. varius* collected in 1976 from western Costa Rica (MVZ149729) is less diverged from an *A. senex* sample collected in the same year approximately 80 km away (MVZ149734) than from

another *A. varius* collected in 1990 (MVZ223280) that was ~250 km away in Eastern Costa Rica (Figure S7). Meanwhile, our fourth Costa Rican sample—*A. chiriquiensis* also collected in 1990 in Eastern Costa Rica (MVZ223270)—lies between the two *A. varius* outgroup samples in the phylogeny (Figure S8). This supports our finding that proximity is a good predictor of genetic divergence in *Atelopus*. While recent studies have made progress clarifying species relationships in this system (Ramírez et al., 2020), a broader genome-wide molecular reanalysis of *Atelopus* from Central America could serve to further clarify these relationships.

4.2 | Preliminary evidence of genetic rescue

“Rescue”, or the reversal in population trajectory for species on the brink of extinction, can be driven by several different underlying processes. Demographic rescue—or simply the increase in number of individuals—may boost population sizes but could leave a species vulnerable to persistent threats (Hufbauer et al., 2015). Genetic rescue, on the other hand, involves an increase in genetic diversity in a population and could potentially facilitate evolutionary rescue by increasing adaptive potential (Whiteley et al., 2015). Genetic rescue can be especially important for imperiled populations that are suffering from reduced N_e . For example, our data show N_e has sharply declined for *A. varius* and that the current N_e estimates for *A. varius* (~40) are similar to other imperiled amphibian populations (e.g., *Ambystoma californiense*, *Rana latastei*; Ficetola et al., 2010; Wang et al., 2011). In this study, we see evidence of demographic rescue and preliminary signs of genetic rescue in one contemporary population of *A. varius*. Additional research will be needed to assess whether these processes lead to evolutionary rescue.

Our strongest evidence for demographic and/or genetic rescue comes from El Copé West—the single population where we found 77% of our contemporary individuals. This contemporary population harbors individuals from three distinct genetic groups (Figure 3b; Figure S5) and genotypes in this population are much more variable than any other population of *A. varius* (Figure 3a; Figure S4). Some of the contemporary individuals have unique genotypes that are minimally represented in the historical sample group, indicating they may be recent migrants and could be contributing to demographic rescue. Furthermore, we see more individuals with high levels of admixture between different genetic groups in the contemporary samples (Figure 3b). However, contemporary individuals in this population do not show an increase in overall heterozygosity, possibly due to low heterozygosity in mated pairs and high overall relatedness within genetic clusters. We recognize that this finding represents a narrow spatial and temporal snapshot of population genetic dynamics in this system. However, El Copé West was the source of 77% of contemporary samples for this study, suggesting that it is a critical example to consider. More work is needed to continue sampling in this area to determine if admixed individuals truly have higher fitness in this environment. By comparing population outcomes from El Copé West

to other surviving populations with non-admixed persisting populations, we can learn more about the potential for genetic rescue to spur recovery in this species.

Given preliminary evidence of genetic rescue in El Copé West, and our finding that strict boundaries separating nearby genetic groups are generally lacking in this system, we argue that assisted gene flow may be an important management strategy. Conservation interventions to increase genetic diversity such as breeding between populations may be especially important. A recent reintroduction attempt of ~500 *A. varius* individuals reared at PARC and released to the wild yielded no survivors (Panama Amphibian Rescue & Conservation Project, 2018). A growing number of studies indicate that genetic diversity is important for *Bd* resistance. One study found that heterozygosity at major histocompatibility complex (MHC) genes was significantly associated with survival in Lowland leopard frogs (*Rana yavapaiensis*) experimentally infected with *Bd* (Savage & Zamudio, 2011). Another recent study of Australian alpine tree frogs (*Litoria verreauxii alpina*) found that individuals with greater genome-wide heterozygosity had a reduced probability of *Bd* infection in the wild (Banks et al., 2019). Future reintroductions for *A. varius* and *A. zeteki* must consider new approaches, such as induced genetic rescue, to address persistent threats and maladapted captive colonies. Otherwise, we risk maintaining captive *A. varius* and *A. zeteki* populations without a clear path forward for successful reintroduction and reestablishment.

4.3 | Candidate genes for future study

The role of the immune system in the host-*Bd* relationship varies widely among amphibian species. For example, transcriptomic studies have found that some susceptible species show an increase in the expression of immune genes when exposed to *Bd* (Ellison et al., 2014; Savage et al., 2020), while others have suppressed or undetectable immune responses (Ellison et al., 2014; Rosenblum et al., 2012). Other studies have shown that *Bd* inhibits lymphocytes, indicating that it actively suppresses host acquired immunity (Fites et al., 2013). In our study, we found several immune-related gene variants associated with contemporary survivors. First, we document associated SNPs in two toll-like receptor genes (TLR1, TLR4). TLR genes are known to recognize fungal pathogens and are essential to the innate immune response (Brightbill et al., 1999; Kaisho & Akira, 2003). Other studies have linked TLR genes to recognizing and responding to *Bd* (Ellison et al., 2014; Kosch et al., 2019; Richmond et al., 2009). Another related gene in our candidate list was a lysosomal-trafficking regulator gene (LYST) which showed a strong signal of association (5 SNPs, 28 kbp F_{ST} sliding window). These genes traffic molecules across cell membranes and are regulators of TLR gene functions (Westphal et al., 2016). In humans, mutations in LYST genes lead to a severe immunodeficiency and can lead to persistent skin infections (Westphal et al., 2016), making this target an intriguing candidate for future studies.

Furthermore, we found a highly associated SNP in a properdin gene related to the complement system. The vertebrate complement system is important in responding to fungal pathogens (Kozel, 1996) and properdin is a positive regulator of the alternative pathway in the complement system (Pillemer et al., 1954). Activating the complement system via properdin may be important for avoiding immunosuppression strategies employed by *Bd* (Ellison et al., 2014). Other immune-related genes with highly associated SNPs were an interferon-induced 35 kDa protein and interferon-induced transmembrane protein 3. Rosenblum et al. (2008) showed a shared up-regulation of interferon-related genes in response to *Bd* infection in a *Rana* and distantly related *Silurana* species. Additionally, Ellison et al. (2014) showed an increase in interferon-related gene expression in *A. zetekii* infected with *Bd*. Interferons boost immune system processes and therefore may be involved in *Bd* response in these *A. varius* populations. Finally, two SNPs in a T-lymphoma invasion and metastasis-inducing protein gene identified in this analysis were also downregulated in the spleen of *A. zetekii* during *Bd* infection (Ellison et al., 2014).

Two intriguing immune-related genes were shared across both the local (only El Copé West) and global (all *A. varius*) comparisons. First, transmembrane protein 131 (TMEM131) is an important regulator of thymocyte proliferation, which are cells responsible for the production of T lymphocytes (Maharzi et al., 2013). Another study of a persistent frog species that suffered *Bd*-related declines in Australia (*Litoria dayi*) also identified a transmembrane protein gene as under strong selection from *Bd* (McKnight et al., 2020). Second, bis(5'-adenosyl)-triphosphatase (ENPP4) is a gene known for its role in facilitating immune response and is involved in "hydrolase activity" (GO:0016787). This GO term was highly expressed in *A. zetekii* that survived *Bd* infection in a previous study (Ellison et al., 2014). Other studies have shown ENPP4 was up-regulated in snails exposed to bacterial molecular patterns (Zhang et al., 2016), and in newts during lens regeneration (Sousounis et al., 2014).

Beyond the immune system, other studies have found that genes associated with maintaining skin integrity and countering *Bd* pathogenesis may also be key to surviving *Bd* (Ellison et al., 2015). Skin integrity is key because *Bd* pathogenesis leading to host death is linked to disruption of skin functions (Voyles et al., 2009). Here we found that two laminin genes (laminin subunit alpha-5 and laminin subunit beta-1) had SNPs that were associated with *Bd* surviving frogs. Laminin is a major component of epithelial basement membranes (Spénlé et al., 2013) and could be important for maintaining skin integrity during *Bd* invasion. Finally, FAHD2, the gene with the most highly associated SNP in this global *A. varius* comparison, is linked to "hydrolase activity" (GO:0016787) as discussed above.

The presence of previously studied, immunologically relevant genes in our candidate list supports previous work showing that immune system processes are important for *Bd* tolerance or resistance in these species (Ellison et al., 2014). Intriguingly, a growing number of studies indicate that an overactivation of the immune system may be linked to *Bd* susceptibility for some species (Ellison et al., 2014;

Savage et al., 2020). We propose that toll-like receptor genes, and others that interact with this immune pathway such as *LYST*, may be key players in mounting an appropriate immune response to *Bd*. Furthermore, we find more evidence that genes linked to hydrolase activity could be important for *Atelopus* exposed to *Bd*. More work is needed to further understand the relationship of these candidate genes with long-term fitness outcomes, including more longitudinal genomic studies of other persisting *Atelopus* species.

5 | CONCLUSIONS

Some natural, relic populations persist despite catastrophic declines and ongoing threats. Studying natural populations of threatened species can provide a window into population processes that may also be important for successful conservation. Here, we shed light on the population genetic structure of *A. varius* and *A. zetekii* in Panamá following dramatic declines from disease. Our data reveal that the species boundary separating *A. varius* and *A. zetekii* is not well supported. We show that geography and distance predict genetic structure of *A. varius* and *A. zetekii* populations, indicating that populations should be managed according to their proximity with other populations, using our characterization of genetic distinctiveness as a guide. We report an intriguing and unique signature of genotypic diversity and recent admixture in one population, indicating genetic rescue may be viable option for conservation interventions in this system. Finally, recognizing the limited sample size of our contemporary dataset, we generated a list of candidate genes that may be associated with *Bd* survival to be considered in future studies. This study offers a new molecular toolkit for studying *Atelopus*, a clade that has suffered massive declines throughout the neotropics, and a model for disentangling the processes that could contribute to species returning from the brink of extinction.

ACKNOWLEDGEMENTS

We thank H. Ross, E. Griffith, K. Zippel, L. Zippel, R. Perez, A. Estrada, J. Morgan, K. Terrell, G. Rios-Sotelo, G. Rosa, K. Charles, A. Levorse, and the Cruz family for help in the field. We thank K. Lundy, S. McDevitt, and L. Smith for help in the lab and T. Linderorth and G. Bradburd for help with data analysis. We thank the Smithsonian Tropical Research Institute for help with permits and the Museum of Vertebrate Zoology for access to collections. We thank two anonymous reviewers for constructive feedback. The authors declare no conflicts of interest.

DATA AVAILABILITY STATEMENT

The raw sequence data that support the findings of this study are openly available in NCBI SRA (PRJNA634906). Additional data that support the findings of this study are openly available in figshare (https://figshare.com/projects/Atelopus_Exome_Capture/82046). Code used to analyze data and make figures openly available on github (<https://github.com/allie128/Atelopus>).

ORCID

Allison Q. Byrne  <https://orcid.org/0000-0002-5366-0673>

REFERENCES

- Altschul, S. F., Madden, T. L., Schäffer, A. A., Zhang, J., Zhang, Z., Miller, W., & Lipman, D. J. (1997). Gapped BLAST and PSI-BLAST: A new generation of protein database search programs. *Nucleic Acids Research*, 25(17), 3389–3402. <https://doi.org/10.1093/nar/25.17.3389>
- Bankevich, A., Nurk, S., Antipov, D., Gurevich, A. A., Dvorkin, M., Kulikov, A. S., Lesin, V. M., Nikolenko, S. I., Pham, S., Prijbelski, A. D., Pyshkin, A. V., Sirotkin, A. V., Vyahhi, N., Tesler, G., Alekseyev, M. A., & Pevzner, P. A. (2012). SPAdes: A new genome assembly algorithm and its applications to single-cell sequencing. *Journal of Computational Biology*, 19(5), 455–477. <https://doi.org/10.1089/cmb.2012.0021>
- Banks, S. C., Scheele, B. C., Macris, A., Hunter, D., Jack, C., & Fraser, C. I. (2019). Chytrid fungus infection in alpine tree frogs is associated with individual heterozygosity and population isolation but not population-genetic diversity. *Frontiers of Biogeography*, 12(1), e43875. <https://doi.org/10.21425/F5FBG43875>
- Barrio-Amorós, C. L., Costales, M., Vieira, J., Osterman, E., Kaiser, H., & Arteaga, A. (2020). Back from extinction: Rediscovery of the harlequin toad *Atelopus mindoensis* Peters, 1973 in Ecuador. *Herpetology Notes*, 13, 325–328.
- Becker, M. H., Walke, J. B., Cikanek, S., Savage, A. E., Mattheus, N., Santiago, C. N., Minbiole, K. P. C., Harris, R. N., Belden, L. K., & Gratwicke, B. (2015). Composition of symbiotic bacteria predicts survival in Panamanian golden frogs infected with a lethal fungus. *Proceedings of the Royal Society B: Biological Sciences*, 282(1805), 20142881. <https://doi.org/10.1098/rspb.2014.2881>
- Bi, K., Linderth, T., Vanderpool, D., Good, J. M., Nielsen, R., & Moritz, C. (2013). Unlocking the vault: Next-generation museum population genomics. *Molecular Ecology*, 22(24), 6018–6032. <https://doi.org/10.1111/mec.12516>
- Bi, K., Vanderpool, D., Singhal, S., Linderth, T., Moritz, C., & Good, J. M. (2012). Transcriptome-based exon capture enables highly cost-effective comparative genomic data collection at moderate evolutionary scales. *BMC Genomics*, 13(1), 403. <https://doi.org/10.1186/1471-2164-13-403>
- Bolger, A. M., Lohse, M., & Usadel, B. (2014). Trimmomatic: A flexible trimmer for Illumina sequence data. *Bioinformatics*, 30(15), 2114–2120. <https://doi.org/10.1093/bioinformatics/btu170>
- Boyle, D. G., Boyle, D. B., Olsen, V., Morgan, J. A. T., & Hyatt, A. D. (2004). Rapid quantitative detection of chytridiomycosis (*Batrachochytrium dendrobatidis*) in amphibian samples using real-time Taqman PCR assay. *Diseases of Aquatic Organisms*, 60(2), 141–148. <https://doi.org/10.3354/dao060141>
- Bradburd, G. S., Coop, G. M., & Ralph, P. L. (2018). Inferring continuous and discrete population genetic structure across space. *Genetics*, 210(1), 33–52. <https://doi.org/10.1534/genetics.118.301333>
- Brightbill, H. D., Libraty, D. H., Krutzik, S. R., Yang, R.-B., Belisle, J. T., Bleharski, J. R., & Smale, S. T. (1999). Host defense mechanisms triggered by microbial lipoproteins through toll-like receptors. *Science*, 285(5428), 732–736. <https://doi.org/10.1126/science.285.5428.732>
- Brown, J. H., & Kodric-Brown, A. (1977). Turnover rates in insular biogeography: Effect of immigration on extinction. *Ecology*, 58(2), 445–449. <https://doi.org/10.2307/1935620>
- Bustamante, H. M., Livo, L. J., & Carey, C. (2010). Effects of temperature and hydric environment on survival of the Panamanian Golden Frog infected with a pathogenic chytrid fungus. *Integrative Zoology*, 5(2), 143–153. <https://doi.org/10.1111/j.1749-4877.2010.00197.x>
- Carlson, S. M., Cunningham, C. J., & Westley, P. A. H. (2014). Evolutionary rescue in a changing world. *Trends in Ecology & Evolution*, 29(9), 521–530. <https://doi.org/10.1016/j.tree.2014.06.005>
- Crawford, A. J., Lips, K. R., & Bermingham, E. (2010). Epidemic disease decimates amphibian abundance, species diversity, and evolutionary history in the highlands of central Panama. *Proceedings of the National Academy of Sciences*, 107(31), 13777–13782. <https://doi.org/10.1073/pnas.0914115107>
- Crump, M. L. (1986). Homing and site fidelity in a neotropical frog, *Atelopus varius* (Bufonidae). *Copeia*, 1986(2), 438–444. <https://doi.org/10.2307/1445001>
- DiRenzo, G. V., Langhammer, P. F., Zamudio, K. R., & Lips, K. R. (2014). Fungal infection intensity and zoospore output of *Atelopus zeteki*, a potential acute chytrid supershedder. *PLoS One*, 9(3), e93356. <https://doi.org/10.1371/journal.pone.0093356>
- Do, C., Waples, R. S., Peel, D., Macbeth, G. M., Tillett, B. J., & Ovenden, J. R. (2014). NeEstimator v2: Re-implementation of software for the estimation of contemporary effective population size (N_e) from genetic data. *Molecular Ecology Resources*, 14(1), 209–214. <https://doi.org/10.1111/1755-0998.12157>
- Ellison, A. R., Savage, A. E., DiRenzo, G. V., Langhammer, P., Lips, K. R., & Zamudio, K. R. (2014). Fighting a losing battle: Vigorous immune response countered by pathogen suppression of host defenses in the chytridiomycosis-susceptible frog *Atelopus zeteki*. *G3: Genes, Genomes, Genetics*, 4(7), 1275–1289. <https://doi.org/10.1534/g3.114.010744>
- Ellison, A. R., Tunstall, T., DiRenzo, G. V., Hughey, M. C., Rebollar, E. A., Belden, L. K., Harris, R. N., Ibáñez, R., Lips, K. R., & Zamudio, K. R. (2015). More than skin deep: Functional genomic basis for resistance to amphibian chytridiomycosis. *Genome Biology and Evolution*, 7(1), 286–298. <https://doi.org/10.1093/gbe/evu285>
- Estrada, A., Gratwicke, B., Benedetti, A., Dellatogna, G., Garrelle, D., Griffith, E., Ibáñez, R., Ryan, S., & Miller, P. (2014). The golden frogs of Panama (*Atelopus zeteki*, *A. varius*): A conservation planning workshop: Final report, 1–102.
- Evanno, G., Regnaut, S., & Goudet, J. (2005). Detecting the number of clusters of individuals using the software STRUCTURE: A simulation study. *Molecular Ecology*, 14(8), 2611–2620. <https://doi.org/10.1111/j.1365-294X.2005.02553.x>
- Ficetola, G. F., Padoa-Schioppa, E., Wang, J., & Garner, T. W. J. (2010). Polygyny, census and effective population size in the threatened frog, *Rana latastei*. *Animal Conservation*, 13(s1), 82–89. <https://doi.org/10.1111/j.1469-1795.2009.00306.x>
- Fites, S., Ramsey, J., Holden, W., Collier, S., Sutherland, D. M., Reinert, L., & Rollins-Smith, L. (2013). The invasive chytrid fungus of amphibians paralyzes lymphocyte responses. *Science*, 342(6156), 366–369. <https://doi.org/10.1021/ja8019214>
- Frankham, R. (2005). Genetics and extinction. *Biological Conservation*, 126(2), 131–140. <https://doi.org/10.1016/j.biocon.2005.05.002>
- Gagliardo, R., Crump, P., Griffith, E., Mendelson, J., Ross, H., & Zippel, K. (2008). The principles of rapid response for amphibian conservation, using the programmes in Panama as an example. *International Zoo Yearbook*, 42(1), 125–135. <https://doi.org/10.1111/j.1748-1090.2008.00043.x>
- Gilpin, M. E., & Soule, M. E. (1986). Minimum viable populations: Processes of species extinction. In: *Conservation biology: The science of scarcity and diversity* (pp. 19–34). Sinauer Associates.
- Gomulkiewicz, R., & Holt, R. D. (1995). When does evolution by natural selection prevent extinction? *Evolution*, 49(1), 201–207. <https://doi.org/10.1111/j.1558-5646.1995.tb05971.x>
- Gonzalez, A., Ronce, O., Ferriere, R., & Hochberg, M. E. (2013). Evolutionary rescue: An emerging focus at the intersection between ecology and evolution. *Philosophical Transactions of the Royal Society B: Biological Sciences*, 368(1610). <https://doi.org/10.1098/rstb.2012.0404>
- González-Maya, J. F., Belant, J. L., Wyatt, S. A., Schipper, J., Cardenal, J., Corrales, D., Cruz-Lizano, I., Hoepker, A., Escobedo-Galván, A. H., Castañeda, F., & Fischer, A. (2013). Renewing hope: The rediscovery

- of *Atelopus varius* in Costa Rica. *Amphibia-Reptilia*, 34, 573–578. <https://doi.org/10.1163/15685381-00002910>
- González-Maya, J. F., Gómez-Hoyos, D. A., Cruz-Lizano, I., & Schipper, J. (2018). From hope to alert: Demography of a remnant population of the Critically Endangered *Atelopus varius* from Costa Rica. *Studies on Neotropical Fauna and Environment*, 53(3), 194–200. <https://doi.org/10.1080/01650521.2018.1460931>
- Goslee, S. C., & Urban, D. L. (2007). The ecodist package for dissimilarity-based analysis of ecological data. *Journal of Statistical Software*, 22(7), 1–19.
- Gotz, S., Garcia-Gomez, J. M., Terol, J., Williams, T. D., Nagaraj, S. H., Nueda, M. J., Robles, M., Talon, M., Dopazo, J., & Conesa, A. (2008). High-throughput functional annotation and data mining with the Blast2GO suite. *Nucleic Acids Research*, 36(10), 3420–3435. <https://doi.org/10.1093/nar/gkn176>
- Grabherr, M. G., Haas, B. J., Yassour, M., Levin, J. Z., Thompson, D. A., Amit, I., Adiconis, X., Fan, L., Raychowdhury, R., Zeng, Q., Chen, Z., Mauceli, E., Hacohen, N., Gnirke, A., Rhind, N., di Palma, F., Birren, B. W., Nusbaum, C., Lindblad-Toh, K., ... Regev, A. (2011). Full-length transcriptome assembly from RNA-Seq data without a reference genome. *Nature Biotechnology*, 29(7), 644–652. <https://doi.org/10.1038/nbt.1883>
- Hedrick, P. W., & Garcia-Dorado, A. (2016). Understanding inbreeding depression, purging, and genetic rescue. *Trends in Ecology & Evolution*, 31(12), 940–952. <https://doi.org/10.1016/j.tree.2016.09.005>
- Huang, X., & Madan, A. (1999). CAP3: A DNA sequence assembly program. *Genome Research*, 9(9), 868–877. <https://doi.org/10.1101/gr.9.9.868>
- Hufbauer, R. A., Szűcs, M., Kasyon, E., Youngberg, C., Koontz, M. J., Richards, C., Tuff, T. Y., & Melbourne, B. A. (2015). Three types of rescue can avert extinction in a changing environment. *Proceedings of the National Academy of Sciences of the United States of America*, 112(33), 10557 LP-10562. <https://doi.org/10.1073/pnas.1504732112>
- Hyatt, A. D., Boyle, D. G., Olsen, V., Boyle, D. B., Berger, L., Obendorf, D., Dalton, A., Kriger, K., Hero, M., Hines, H., Phillott, R., Campbell, R., Marantelli, G., Gleason, F., & Colling, A. (2007). Diagnostic assays and sampling protocols for the detection of *Batrachochytrium dendrobatidis*. *Diseases of Aquatic Organisms*, 73(3), 175–192. <https://doi.org/10.3354/dao073175>
- Ingvansson, P. K. (2001). Restoration of genetic variation lost – The genetic rescue hypothesis. *Trends in Ecology & Evolution*, 16(2), 62–63. [https://doi.org/10.1016/S01695347\(00\)02065-6](https://doi.org/10.1016/S01695347(00)02065-6)
- Jacquard, A. (1974). *The genetic structure of populations* (Vol. 5). Springer Science & Business Media.
- Jones, O. R., & Wang, J. (2010). COLONY: A program for parentage and sibship inference from multilocus genotype data. *Molecular Ecology Resources*, 10(3), 551–555. <https://doi.org/10.1111/j.1755-0998.2009.02787.x>
- Jónsson, H., Ginolhac, A., Schubert, M., Johnson, P. L. F., & Orlando, L. (2013). mapDamage2.0: Fast approximate Bayesian estimates of ancient DNA damage parameters. *Bioinformatics*, 29(13), 1682–1684. <https://doi.org/10.1093/bioinformatics/btt193>
- Kaisho, T., & Akira, S. (2003). Regulation of dendritic cell function through Toll-like receptors. *Current Molecular Medicine*, 3(8), 759–771. <https://doi.org/10.2174/1566524033479366>
- Kopelman, N. M., Mayzel, J., Jakobsson, M., Rosenberg, N. A., & Mayrose, I. (2015). Clumpak: A program for identifying clustering modes and packaging population structure inferences across K. *Molecular Ecology Resources*, 15(5), 1179–1191. <https://doi.org/10.1111/1755-0998.12387>
- Korneliussen, T. S., Albrechtsen, A., & Nielsen, R. (2014). ANGSD: Analysis of next generation sequencing data. *BMC Bioinformatics*, 15(1), <https://doi.org/10.1186/s12859-014-0356-4>
- Korneliussen, T. S., & Moltke, I. (2015). NgsRelate: A software tool for estimating pairwise relatedness from next-generation sequencing data. *Bioinformatics*, 31(24), 4009–4011. <https://doi.org/10.1093/bioinformatics/btv509>
- Korneliussen, T. S., Moltke, I., Albrechtsen, A., & Nielsen, R. (2013). Calculation of Tajima's D and other neutrality test statistics from low depth next-generation sequencing data. *BMC Bioinformatics*, 14(1), 289. <https://doi.org/10.1186/1471-2105-14-289>
- Kosch, T. A., Silva, C. N. S., Brannelly, L. A., Roberts, A. A., Lau, Q., Marantelli, G., Berger, L., & Skerratt, L. F. (2019). Genetic potential for disease resistance in critically endangered amphibians decimated by chytridiomycosis. *Animal Conservation*, 22(3), 238–250. <https://doi.org/10.1111/acv.12459>
- Kozel, T. R. (1996). Activation of the complement system by pathogenic fungi. *Clinical Microbiology Reviews*, 9(1), 34 LP-46. <https://doi.org/10.1128/CMR.9.1.34>
- La Marca, E., Lips, K. R., Lötters, S., Puschendorf, R., Ibáñez, R., Rueda-Almonacid, J. V., & Young, B. E. (2005). Catastrophic population declines and extinctions in neotropical harlequin frogs (Bufonidae, *Atelopus*). *Biotropica*. Blackwell Publishing Ltd. <https://doi.org/10.1111/j.1744-7429.2005.00026.x>
- Lefort, V., Desper, R., & Gascuel, O. (2015). FastME 2.0: A comprehensive, accurate, and fast distance-based phylogeny inference program. *Molecular Biology and Evolution*, 32(10), 2798–2800. <https://doi.org/10.1093/molbev/msv150>
- Lewis, C. H. R., Richards-Zawacki, C. L., Ibáñez, R., Luedtke, J., Voyles, J., Houser, P., & Gratwicke, B. (2019). Conserving Panamanian harlequin frogs by integrating captive-breeding and research programs. *Biological Conservation*, 236, 180–187. <https://doi.org/10.1016/j.biocon.2019.05.029>
- Li, W., & Godzik, A. (2006). Cd-hit: A fast program for clustering and comparing large sets of protein or nucleotide sequences. *Bioinformatics*, 22(13), 1658–1659. <https://doi.org/10.1093/bioinformatics/btl158>
- Li, H., Handsaker, B., Wysoker, A., Fennell, T., Ruan, J., Homer, N., Marth, G., Abecasis, G., & Durbin, R. (2009). The sequence alignment/map format and SAMtools. *Bioinformatics*, 25(16), 2078–2079. <https://doi.org/10.1093/bioinformatics/btp352>
- Longcore, J. E., Pessier, A. P., & Nichols, D. K. (1999). *Batrachochytrium dendrobatidis* gen. et sp. nov., a chytrid pathogenic to amphibians. *Mycologia*, 91(2), 219–227. <https://doi.org/10.2307/3761366>
- Magoč, T., & Salzberg, S. L. (2011). FLASH: Fast length adjustment of short reads to improve genome assemblies. *Bioinformatics*, 27(21), 2957–2963. <https://doi.org/10.1093/bioinformatics/btr507>
- Maharzi, N., Parietti, V., Nelson, E., Denti, S., Robledo-Sarmiento, M., Setterblad, N., Parcelier, A., Pla, M., Sigaux, F., Gluckman, J. C., & Canque, B. (2013). Identification of TMEM131L as a novel regulator of thymocyte proliferation in humans. *The Journal of Immunology*, 190(12), 6187 LP-6197. <https://doi.org/10.4049/jimmunol.1300400>
- Martin, M. (2011). Cutadapt removes adapter sequences from high-throughput sequencing reads. *EMBnet journal*, 17(1), 10–12. <https://doi.org/10.14806/ej.17.1.200>
- McKenna, A., Hanna, M., Banks, E., Sivachenko, A., Cibulskis, K., Kernysky, A., Garimella, K., Altshuler, D., Gabriel, S., Daly, M., & DePristo, M. A. (2010). The genome analysis toolkit: A mapReduce framework for analyzing next-generation DNA sequencing data. *Genome Research*, 20(9), 1297–1303. <https://doi.org/10.1101/gr.107524.110>
- McKnight, D. T., Carr, L. J., Bower, D. S., Schwarzkopf, L., Alford, R. A., & Zenger, K. R. (2020). Infection dynamics, dispersal, and adaptation: Understanding the lack of recovery in a remnant frog population following a disease outbreak. *Heredity*, 125, 110–123. <https://doi.org/10.1038/s41437-020-0324-x>
- Meisner, J., & Albrechtsen, A. (2018). Inferring population structure and admixture proportions in low-depth NGS data. *Genetics*, 210(2), 719 LP-731. <https://doi.org/10.1534/genetics.118.301336>
- Mitchell, A., Chang, H.-Y., Daugherty, L., Fraser, M., Hunter, S., Lopez, R., McAnulla, C., McMenamin, C., Nuka, G., Pesseat, S., Sangrador-Vegas, A., Scheremetjew, M., Rato, C., Yong, S.-Y., Bateman, A., Punta, M., Attwood, T. K., Sigrist, C. J. A., Redaschi, N., ... Finn, R. D. (2014). The InterPro protein families database: The classification

- resource after 15 years. *Nucleic Acids Research*, 43(D1), D213–D221. <https://doi.org/10.1093/nar/gku1243>
- Moritz, C. (1994). Defining “evolutionarily significant units” for conservation. *Trends in Ecology & Evolution*, 9(10), 373–375. [https://doi.org/10.1016/0169-5347\(94\)90057-4](https://doi.org/10.1016/0169-5347(94)90057-4)
- Nielsen, R., Paul, J. S., Albrechtsen, A., & Song, Y. S. (2011). Genotype and SNP calling from next-generation sequencing data. *Nature Reviews Genetics*, 12(6), 443–451. <https://doi.org/10.1038/nrg2986>
- Panama Amphibian Rescue and Conservation Project. (2018). 2018 Annual Report. Retrieved from <https://parcplace.org/wp-content/uploads/2019/01/PARC-2018-FINAL.pdf>
- Panama Amphibian Rescue and Conservation Project. (2019). 2019 Annual Report. Retrieved from <https://parcplace.org/wp-content/uploads/2020/02/2019-Annual-Report.pdf>
- Perez, R., Richards-zawacki, C. L., Krohn, A. R., Robak, M., Griffith, E. J., Ross, H., & Voyles, J. (2014). Field surveys in Western Panama indicate populations of *Atelopus varius* frogs are persisting in regions where *Batrachochytrium dendrobatidis* is now enzootic. *Amphibian & Reptile Conservation*, 8(2), 30–35.
- Pillemer, L., Blum, L., Lepow, I. H., Ross, O. A., Todd, E. W., & Wardlaw, A. C. (1954). The properdin system and immunity: I. Demonstration and isolation of a new serum protein, properdin, and its role in immune phenomena. *Science*, 120(3112), 279–285. Retrieved from <http://www.jstor.org/stable/1682494>
- Poole, V. (2008). Project golden frog. *Endangered Species Update*, 25(1), S7.
- Ramírez, J. P., Jaramillo, C. A., Lindquist, E. D., Crawford, A. J., & Ibáñez, R. (2020). Recent and rapid radiation of the highly endangered harlequin frogs (*Atelopus*) into Central America inferred from mitochondrial DNA sequences. *Diversity*, 12(9), 360. <https://doi.org/10.3390/d12090360>
- Richards, C. L., & Knowles, L. L. (2007). Tests of phenotypic and genetic concordance and their application to the conservation of Panamanian golden frogs (*Anura*, *Bufo*idae). *Molecular Ecology*, 16(15), 3119–3133. <https://doi.org/10.1111/j.1365-294X.2007.03369.x>
- Richmond, J. Q., Savage, A. E., Zamudio, K. R., & Rosenblum, E. B. (2009). Toward immunogenetic studies of amphibian chytridiomycosis: Linking innate and acquired immunity. *BioScience*, 59(4), 311–320. <https://doi.org/10.1525/bio.2009.59.4.9>
- Rio, D. C., Ares, M., Hannon, G. J., & Nilsen, T. W. (2010). Purification of RNA using TRIzol (TRI reagent). *Cold Spring Harbor Protocols*, 2010(6), pdb-prot5439. <https://doi.org/10.1101/pdb.prot5439>
- Rodríguez-Contreras, A., Señaris, J. C., Lampo, M., & Rivero, R. (2008). Rediscovery of *Atelopus cruciger* (*Anura*: *Bufo*idae): Current status in the Cordillera de La Costa. *Venezuela. Oryx*, 42(2), 301–304. <https://doi.org/10.1017/S0030605308000082>
- Rosenblum, E. B., Poorten, T. J., Settles, M., & Murdoch, G. K. (2012). Only skin deep: Shared genetic response to the deadly chytrid fungus in susceptible frog species. *Molecular Ecology*, 21(13), 3110–3120. <https://doi.org/10.1111/j.1365-294X.2012.05481.x>
- Rosenblum, E. B., Stajich, J. E., Maddox, N., & Eisen, M. B. (2008). Global gene expression profiles for life stages of the deadly amphibian pathogen *Batrachochytrium dendrobatidis*. *Proceedings of the National Academy of Sciences of the United States of America*, 105(44), 17034–17039. <https://doi.org/10.1073/pnas.0804173105>
- Savage, A. E., Gratwicke, B., Hope, K., Bronikowski, E., & Fleischer, R. C. (2020). Sustained immune activation is associated with susceptibility to the amphibian chytrid fungus. *Molecular Ecology*, 29(15), 2889–2903. <https://doi.org/10.1111/mec.15533>
- Savage, A. E., & Zamudio, K. R. (2011). MHC genotypes associate with resistance to a frog-killing fungus. *Proceedings of the National Academy of Sciences of the United States of America*, 108(40), 16705–16710. <https://doi.org/10.1073/pnas.1106893108>
- Savage, J. M. (1972). The harlequin frogs, genus *Atelopus*, of Costa Rica and Western Panama. *Herpetologica*, 28(2), 77–94. Retrieved from <http://www.jstor.org/stable/3891084>
- Schroeder, A., Mueller, O., Stocker, S., Salowsky, R., Leiber, M., Gassmann, M., & Ragg, T. (2006). The RIN: An RNA integrity number for assigning integrity values to RNA measurements. *BMC Molecular Biology*, 7(1), 1–14. <https://doi.org/10.1186/1471-2199-7-3>
- Shaffer, M. L. (1981). Minimum population sizes for species conservation. *BioScience*, 31(2), 131–134. <https://doi.org/10.2307/1308256>
- Singhal, S. (2013). De novo transcriptomic analyses for non-model organisms: An evaluation of methods across a multi-species data set. *Molecular Ecology Resources*, 13(3), 403–416. <https://doi.org/10.1111/1755-0998.12077>
- Skotte, L., Korneliussen, T. S., & Albrechtsen, A. (2013). Estimating individual admixture proportions from next generation sequencing data. *Genetics*, 195(3), 693–702. <https://doi.org/10.1534/genetics.113.154138>
- Slater, G. S. C., & Birney, E. (2005). Automated generation of heuristics for biological sequence comparison. *BMC Bioinformatics*, 6(1), 31. <https://doi.org/10.1186/1471-2105-6-31>
- Sousounis, K., Bhavsar, R., Looso, M., Krüger, M., Beebe, J., Braun, T., & Tsonis, P. A. (2014). Molecular signatures that correlate with induction of lens regeneration in newts: Lessons from proteomic analysis. *Human Genomics*, 8(1), 22. <https://doi.org/10.1186/s40246-014-0022-y>
- Spenlé, C., Simon-Assmann, P., Orend, G., & Miner, J. H. (2013). Laminin $\alpha 5$ guides tissue patterning and organogenesis. *Cell Adhesion & Migration*, 7(1), 90–100. <https://doi.org/10.4161/cam.22236>
- Tallmon, D. A., Luikart, G., & Waples, R. S. (2004). The alluring simplicity and complex reality of genetic rescue. *Trends in Ecology & Evolution*, 19(9), 489–496. <https://doi.org/10.1016/j.tree.2004.07.003>
- Tapia, E. E., Coloma, L. A., Pazmiño-Otamendi, G., & Peñafiel, N. (2017). Rediscovery of the nearly extinct longnose harlequin frog *Atelopus longirostris* (*Bufo*nidae) in Junín, Imbabura, Ecuador. *Neotropical Biodiversity*, 3(1), 157–167. <https://doi.org/10.1080/23766808.2017.1327000>
- Vieira, F. G., Lassalle, F., Korneliussen, T. S., & Fumagalli, M. (2016). Improving the estimation of genetic distances from Next-Generation Sequencing data. *Biological Journal of the Linnean Society*, 117(1), 139–149. <https://doi.org/10.1111/bij.12511>
- Voyles, J., Woodhams, D. C., Saenz, V., Byrne, A. Q., Perez, R., Rios-Sotelo, G., Ryan, M. J., Bletz, M. C., Sobell, F. A., McLetchie, S., Reinert, L., Rosenblum, E. B., Rollins-Smith, L. A., Ibáñez, R., Ray, J. M., Griffith, E. J., Ross, H., & Richards-Zawacki, C. L. (2018). Shifts in disease dynamics in a tropical amphibian assemblage are not due to pathogen attenuation. *Science*, 359(6383), 1517–1519. <https://doi.org/10.1126/science.aao4806>
- Voyles, J., Young, S., Berger, L., Campbell, C., Voyles, W. F., Dinudom, A., Cook, D., Webb, R., Alford, R. A., Skerratt, L. F., & Speare, R. (2009). Pathogenesis of chytridiomycosis, a cause of catastrophic amphibian declines. *Science*, 326(5952), 582–585. <https://doi.org/10.1126/science.1176765>
- Wang, I. J., Johnson, J. R., Johnson, B. B., & Shaffer, H. B. (2011). Effective population size is strongly correlated with breeding pond size in the endangered California tiger salamander, *Ambystoma californiense*. *Conservation Genetics*, 12(4), 911–920. <https://doi.org/10.1007/s10592-011-0194-0>
- Wang, J. (2009). A new method for estimating effective population sizes from a single sample of multilocus genotypes. *Molecular Ecology*, 18(10), 2148–2164. <https://doi.org/10.1111/j.1365-294X.2009.04175.x>
- Weir, B. S., & Cockerham, C. C. (1984). Estimating F-statistics for the analysis of population structure. *Evolution*, 38(6), 1358–1370.
- Westphal, A., Cheng, W., Yu, J., Grassl, G., Krautkrämer, M., Holst, O., Föger, N., & Lee, K.-H. (2016). Lysosomal trafficking regulator Lyst links membrane trafficking to toll-like receptor-mediated inflammatory responses. *Journal of Experimental Medicine*, 214(1), 227–244. <https://doi.org/10.1084/jem.20141461>
- Whiteley, A. R., Fitzpatrick, S. W., Funk, W. C., & Tallmon, D. A. (2015). Genetic rescue to the rescue. *Trends in Ecology & Evolution*, 30(1), 42–49. <https://doi.org/10.1016/j.tree.2014.10.009>

- Woodhams, D. C., Voyles, J., Lips, K. R., Carey, C., & Rollins-Smith, L. A. (2006). Predicted disease susceptibility in a Panamanian amphibian assemblage based on skin peptide defenses. *Journal of Wildlife Diseases*, 42(2), 207–218. <https://doi.org/10.7589/0090-3558-42.2.207>
- Zhang, S.-M., Loker, E. S., & Sullivan, J. T. (2016). Pathogen-associated molecular patterns activate expression of genes involved in cell proliferation, immunity and detoxification in the amebocyte-producing organ of the snail *Biomphalaria glabrata*. *Developmental & Comparative Immunology*, 56, 25–36. <https://doi.org/10.1016/j.dci.2015.11.008>
- Zippel, K. C., Ibáñez, R., Lindquist, E. D., Richards, C. L., Jaramillo, C. A., & Griffith, E. J. (2006). Implicaciones en la conservación de las ranas doradas de Panamá, asociadas con su revisión taxonómica. *Herpetologicos*, 3(1), 29–39.

SUPPORTING INFORMATION

Additional supporting information may be found online in the Supporting Information section.

How to cite this article: Byrne AQ, Richards-Zawacki CL, Voyles J, Bi K, Ibáñez R, Rosenblum EB. Whole exome sequencing identifies the potential for genetic rescue in iconic and critically endangered Panamanian harlequin frogs. *Glob Change Biol.* 2020;00:1–21. <https://doi.org/10.1111/gcb.15405>